Dear Author,

Please, note that changes made to the HTML content will be added to the article before publication, but are not reflected in this PDF.

Note also that this file should not be used for submitting corrections.

Earth-Science Reviews xxx (2015) xxx–xxx

Contents lists available at ScienceDirect

Earth-Science Reviews

journal homepage: www.elsevier.com/locate/earscirev

Comparison between *single-event effects* and *cumulative effects* for the purpose of seismic hazard assessment. A review from Greece

R. Caputo [a,b], S. Sboras [c], S. Pavlides [d,b], A. Chatzipetros [d,b]

[a] *Department of Physics and Earth Sciences, University of Ferrara, Italy*
[b] *Research & Teaching Centre for Earthquake Geology, Tyrnavos, Greece*
[c] *National Centre for Environment and Sustainable Development, National Observatory of Athens, Greece*
[d] *Department of Geology, Aristotle University of Thessaloniki, Greece*

ARTICLE INFO

Article history:
Received 26 February 2015
Accepted 8 May 2015
Available online xxxx

Keywords:
Active faults
Morphotectonics
Seismotectonics
Sources of information
Earthquake geology

ABSTRACT

When compiling a database of active and capable faults, or more in general when collecting data for Seismic Hazard Assessment (SHA) purposes, the exploitation of the numerous and different *sources of information* represents a crucial issue. Also the understanding of their potential and limitations is essential. For example, using only information deriving from historically and/or instrumentally recorded earthquakes, as it has been commonly applied in the past, it is not sufficient and it could be, sometimes, even misleading in terms of SHA. In the present paper, the importance of using geological information for better defining the principal seismotectonic parameters of a seismogenic source is discussed and emphasized. In order to show this, four case studies of active faults recently reactivated by strong earthquakes have been selected from the Greek Database of Seismogenic Sources (GreDaSS). Each seismogenic source is analysed twice and separately for the two *sources of information*: firstly, on the basis of the *single-event effects* as mainly provided by historically or instrumentally recorded data, and secondly, on the basis of the *cumulative effects* consisting of any, mainly geological, evidence caused by multiple and repeated fault reactivations of the specific seismogenic source. The quality and accuracy of the produced results from both *sources of information* are then discussed in order to define the reliability of the outcomes and especially for calibrating the methodological approaches based on geological data, which have not only an intrinsically different degree of uncertainty and resolution, but also a greater potential in exploitability. As a matter of fact, an improved geological, in its broader sense, knowledge will help to fill in the gap of the geodetically and/or seismologically determined tectonic activity of hazardous regions. Moreover, including also in a catalogue the seismogenic sources that are not associated with historical and/or instrumental earthquakes will have a remarkable impact in future SHA analyses either probabilistic or deterministic ones.

Contents

E-mail address: rcaputo@unife.it (R. Caputo).

http://dx.doi.org/10.1016/j.earscirev.2015.05.004
0012-8252/© 2015 Published by Elsevier B.V.

1. Introduction

Large earthquakes often attract the interest of many researchers and consequently the literature corresponding to the causative faults becomes rich and abundant. Among the several reasons for this particular attention devoted by the scientific community there is the need of i) soon investigating the evanescent co-seismic ruptures and other secondary effects, ii) improving the SHA of the affected areas, iii) better understanding the reactivated tectonic structure and the broader geodynamic processes undergoing at a larger scale and iv) exporting the collected information to similar geological and tectonic settings. On the other hand, silent faults and/or minor earthquakes are much less analysed or they are generally investigated at a broad regional scale with different methodological approaches. This discrepancy has two effects on the collected information of potential seismogenic faults that have not been recently (viz. historically) reactivated: firstly, data are scattered and sometimes 'hidden' in various studies and hence difficult to be mined; secondly, data are sometimes inconsistent because of deriving from the application of not always proper investigation methods. On the other hand, consistency and uniformity of information represent a crucial issue for enabling the comparison between seismogenic sources at a regional scale and especially for SHA analyses.

The early efforts of systematic collection of seismogenic sources for Greece and surroundings were focused on faults that were related to either historically or instrumentally recorded earthquakes. For example, Ambraseys and Jackson (1998) have listed and analysed historical and instrumental events associated with surface faulting that occurred in the East Mediterranean, while Papazachos et al. (1999) compiled a map of 'rupture zones' representing seismogenic volumes responsible for the recent events affecting the broader Aegean Region. It is noteworthy that both papers were almost exclusively based on historical and instrumental seismological data.

During the same period, the first parametric databases of active faults were compiled for Italy (Valensise and Pantosti, 2001) and Southern Europe (FAUST, 2001), including *ca.* 50 sources for the Aegean Region. Although these were the first databases including all principal seismotectonic parameters, most seismogenic sources were associated with recently reactivated faults, with few exceptions where geological information was also considered.

A step forward in the direction of including also geological information is represented by the map of capable faults in Greece and the broader Aegean Region compiled by Pavlides et al. (2007), which includes all fault scarps and traces with a clear morphological expression meeting one or more of the criteria commonly used for identifying active faults (e.g. Burbank and Anderson, 2001; Bull, 2009; McCalpin, 2009). As an innovative result, most of the faults included in the map are not related with known earthquakes. However, a strong limitation of this map is the lack of any parametric information except for the geographical ones, which makes it of little use for SHA analyses.

More recently, Karakaisis et al. (2010) provide a re-assessment of previous seismologically-based compilations (Papazachos et al., 1999), whereas Mountrakis et al. (2006) using geological and seismological evidences present an interesting review of active faults though limited to a small sector of northern Greece (from Rhodope to West Macedonia). Additionally and like other similar 'local' compilations, these works are generally rather descriptive without quantitative parametric information.

In summary, past inventories of seismogenic sources for the Aegean Region either show the paucity of crucial seismotectonic information or are unsatisfactory in terms of completeness of seismogenic sources. On the one side, neotectonic maps do not contain any other parametric data except the geographic ones; on the other hand, the seismologically-based catalogues generally provide additional information relative to some geometric and kinematic parameters, but are largely deficient especially as concerns the number of recognised capable faults, which are probably the potential seismogenic sources of more concern for SHA analyses.

In order to carry out more realistic and reliable SHA analyses, the importance and the need of systematically parameterizing active and capable faults within Mediterranean and other European seismogenic regions were definitely realized during the last decade (e.g. DISS WG, 2010; Basili et al., 2013; Lunina et al., 2014). Similarly motivated is the GreDaSS (Greek Database of Seismogenic Sources) Project (Caputo and Pavlides, 2013) devoted to create a fully parametric repository of potential seismogenic sources ($M_w > 5.5$) for the broader Aegean Region (Fig. 1). Like all open-files of this kind, research activities in the frame of the GreDaSS Project are still in progress (Pavlides et al., 2010; Caputo et al., 2012; Sboras et al., 2014). Q12

The principal aim of this paper is not to present and describe GreDaSS or its rationale, neither its informatic structure kindly provided by the DISS WG (see Basili et al. (2008) and references therein), but to focus on some crucial methodological issues and problems which are commonly coped with during such compilation works including GreDaSS.

For the purpose of this paper, firstly, we review the different *sources of information* that could potentially provide a useful input for this kind of databases and, secondly, we present and discuss four case studies from GreDaSS (Fig. 1). In particular, we will focus on four *individual seismogenic sources* (ISSs) which are characterized by a full set of geometric (geographic fault location, strike, dip, length, width, minimum and maximum depth), kinematic (rake and slip-per-event), dynamic (maximum expected magnitude) and chronological parameters (date of last major earthquake, slip-rate and mean recurrence interval) (Fig. 2 and Table 1). ISSs are implicitly assumed to behave according to a characteristic earthquake model (Schwartz and Coppersmith, 1984), though it can be seldom documented to be the real case for Mediterranean active faults. In order to overcome this problem, whose discussion is however well beyond the goals of this paper, since several years the *composite seismogenic sources*, CSSs, have been introduced in databases like GreDaSS (Caputo and Pavlides, 2013), DISS (DISS WG, 2010) and EDSF (Basili et al., 2013). The latter represent generally broader tectonic structures which are not assumed to be capable of a specific-size earthquake, but their seismic potential (viz. maximum expected magnitude) can be estimated from existing earthquake catalogues or based on geological and seismotectonic considerations. The introduction of the CSSs effectively enhanced the completeness of potential seismogenic sources included in these databases, although this may imply a smaller accuracy in their description.

2. Two different *sources of information*

It is worth mentioning that the creation of a parametric database of potential seismogenic sources like GreDaSS (Caputo and Pavlides, 2013), essentially stands on the systematic collection and critical analysis of all available information which could enable to quantify the

Please cite this article as: Caputo, R., et al., Comparison between *single-event effects* and *cumulative effects* for the purpose of seismic hazard assessment. A review from Greece, Earth-Sci. Rev. (2015), http://dx.doi.org/10.1016/j.earscirev.2015.05.004

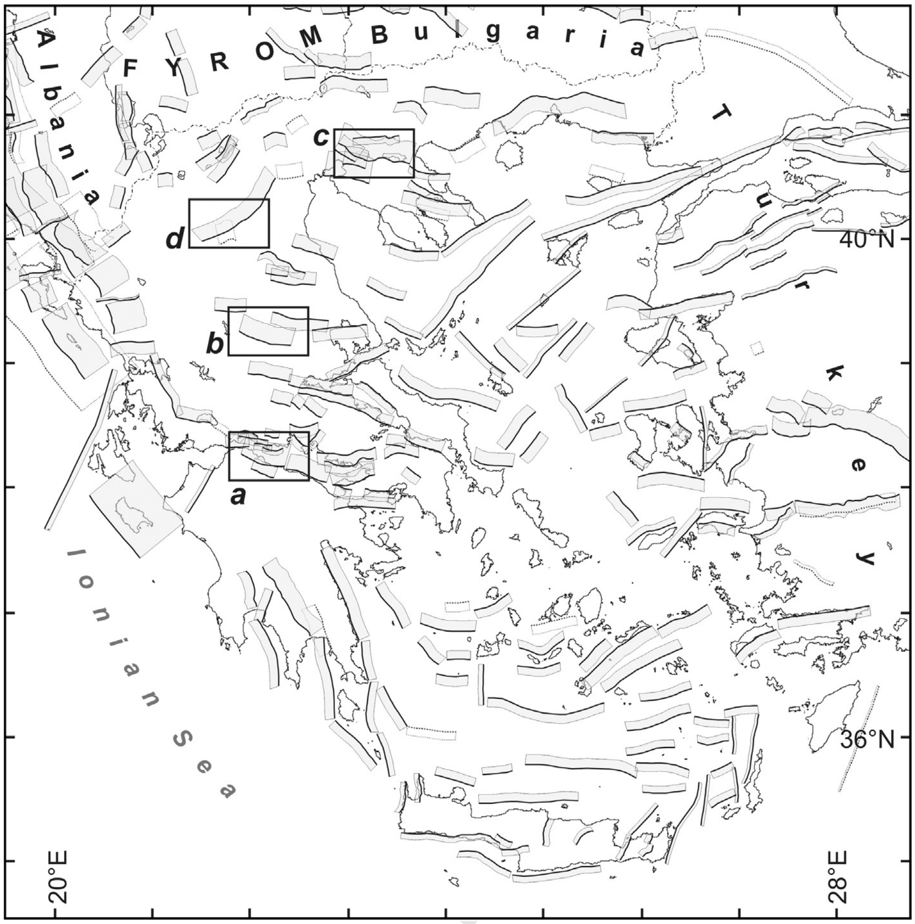

Fig. 1. Seismotectonic map of the Aegean Region showing the *composite seismogenic sources* (CSSs) included in GreDaSS (Caputo and Pavlides, 2013). Black boxes indicate the four case studies containing the *individual seismogenic sources* (ISSs) considered and discussed in the present paper (a: 1861 Valimitika earthquake and South Gulf of Corinth Fault System; b: 1954 Sophades earthquake and Domokos Fault System; c: 1978 Stivos earthquake and Mygdonia Fault System; d: 1995 Kozani–Grevena earthquake and Aliakmonas Fault System).

principal seismotectonic parameters (Fig. 2 and Table 1; Basili et al., 2008). As mentioned above, the first databases of this type for Italy and Greece (e.g. FAUST, 2001; Valensise and Pantosti, 2001) included almost exclusively faults unquestionably associated with historical and instrumental earthquakes (M > 5.5). Indeed, Historical Seismology for these two countries was already quite advanced at that time (Galanopoulos, 1960, 1961; Postpischl, 1985; Guidoboni, 1989; Papazachos and Papazachou, 1989, 1997; Ambraseys and Jackson, 1990; 1998; Guidoboni et al., 1994; Boschi et al., 1997; Camassi and Stucchi, 1997; Ambraseys, 2001; Stucchi et al., 2001), while earthquake catalogues from the seismological networks of the Aristotle University of Thessaloniki (http://geophysics.geo.auth.gr/ss/), the National Observatory of Athens (http://www.gein.noa.gr/services/cat.html) and the Istituto Nazionale di Geofisica e Vulcanologia (http://csi.rm.ingv.it/; http://www.bo.ingv.it/RCMT/) were also available.

It is worthless to stress that the more intensely investigated faults were those related with the strongest seismic events that generally occurred during the few past decades, that is to say during the instrumental

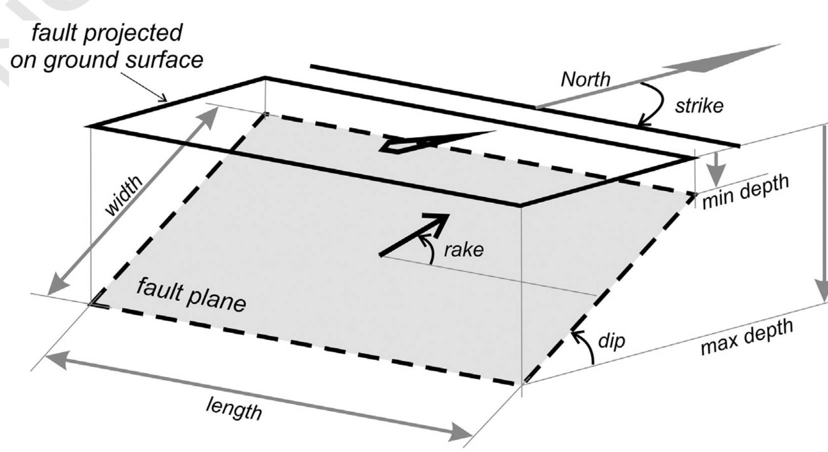

Fig. 2. Schematic representation of an *individual seismogenic source* (ISS) and corresponding geometric and kinematic parameters listed in Table 1. Redrawn from Basili et al. (2008).

Table 1
Synthetic table showing the numerical values obtained from the analysis of *single-event effects* ("s.e.e." columns) and *cumulative effects* ("c.e." columns) for the four case studies. For the definition of each parameter see Fig. 2 and Basili et al. (2008). Numerical values for 'location' are not reported here but graphically shown in the corresponding figures. A qualitative index shown in parentheses, from "A" (greater accuracy and/or lowest uncertainty) to "E" (lowest reliability and/or largest uncertainty), is attributed to each numerical value and indicated in brackets. The "elapsed time" is conventionally considered from last event to 2000 AD.

	South Corinth Fault System		Domokos Fault System			Mygdonia Fault System		Aliakmonas Fault System	
Source of information	*s.e.e.*	*c.e.*	*s.e.e.*	*s.e.e.*	*c.e.*	*s.e.e.*	*c.e.*	*s.e.e.*	*c.e.*
Location	Box *A* (B)	Box *B* (A)	Box *A* (C)	Box *B* (D)	Box *C* (B)	Box *A* (A)	Box *B* (A)	Box *A* (B)	Box *E* (B)
Length [km]	15 (D)	25 (B)	23 (C)	25 (E)	30 (B)	24 (B)	23 (B)	26 (B)	33 (B)
Width [km]	12 (E)	15.5 (C)	16 (D)	15 (E)	17 (C)	16 (B)	18 (C)	18 (C)	20 (C)
Min depth [km]	0 (A)	0 (A)	1 (C)	0 (C)	0 (A)	0 (A)	0 (A)	1 (C)	0 (A)
Max depth [km]	10 (E)	10 (C)	15 (E)	7.5 (E)	15 (C)	12 (B)	15 (B)	14 (A)	15 (B)
Strike [deg]	280 (B)	277 (A)	295 (C)	353 (D)	285 (A)	280 (B)	265 (B)	246 (A)	242 (B)
Dip [deg]	60 (D)	40 (C)	60 (D)	29 (D)	60 (C)	49 (B)	57 (B)	42 (B)	45 (B)
Rake [deg]	270 (D)	280 (B)	270 (E)	300 (D)	285 (B)	286 (B)	280 (C)	264 (B)	265 (C)
Slip per event [m]	1.0 (C)	0.80 (B)	1.0 (C)	0.9 (B)	1.0 (C)	0.5 (B)	0.5 (C)	0.7 (B)	0.5 (D)
Slip-rate [mm/a]	n.a.	0.5–2.0 (C)	n.a.	n.a.	0.3–1.0 (B)	n.a.	0.3–0.7 (B)	n.a.	0.01–0.3 (D)
Recurrence [ka]	n.a.	0.2–1.6 (D)	n.a.	n.a.	>3.2 (C)	n.a.	1.0–1.5 (B)	n.a.	2–10 (D)
Maximum expected magnitude [M_w]	6.6 (C)	6.6 (B)	6.7 (C)	6.7 (C)	6.8 (C)	6.6 (B)	6.5 (C)	6.6 (A)	6.7 (B)
Last ethq [AD]	1861 (A)	>1300 (D)	1954 (A)	1954 (A)	>500 (D)	1978 (A)	>1500 (D)	1995 (A)	>5 ka BP (E)
Elapsed time [years]	139 (A)	<600 (D)	46 (A)	46 (A)	<1500 (E)	22 (A)	<570 (D)	5 (A)	<5 ka (E)

recording period. As a matter of fact, the quantity and quality of seismological information obtained either from major events or microseismic sequences progressively increase with the increasing density of the seismographic networks and the used instrumental technology. For example, recent instrumental data commonly provide more precise seismological constraints, with respect to the past, about the focal depth, magnitude, nodal planes and aftershock distributions, therefore improving our knowledge on the geometry and kinematics of the source.

Also pre-instrumental earthquakes could provide important information relative to seismogenic sources for the aim of compiling a parametric database. However, incompleteness, ambiguity and lack of precision rapidly increases with the age of the event. In practice, for most earthquakes before the 19th century, the information that could be possibly obtained is quite limited and poor in terms of seismotectonic parameters. It is noteworthy that also during the instrumental period, which is not longer than *ca.* 100 years, accuracy in the Aegean Region started to be significant only after the 1970s, when the Greek seismographic network was regionally expanded and technically improved.

The repeated 'surprises' in location and/or magnitude of recent earthquakes, like the 1995 Kozani and 1999 Athens events for Greece, but also the 2001 Bhuj for India, the 2002 San Giuliano di Puglia for Italy, the 2003 Bam for Iran, the 2010 Yushu for Eastern Tibet, the 2004 Sumatra–Andaman for Indonesia, the 2011 Van for Turkey, the 2011 Tohoku for Japan, the 2011 Christchurch for New Zealand (e.g. Lekkas, 2001; Mucciarelli, 2005; Hanks et al., 2012; Li et al., 2012; Wyss et al., 2012; Kagan and Jackson, 2013; Mulargia, 2013; Utkucu, 2013; Silverii et al., 2014; Steacy et al., 2014; and many other), made the scientific community aware that the creation of a database of potential seismogenic sources to be used in SHA analyses cannot be based solely on the analysis of instrumental and historical events and correlated information. Among the several motivations for searching alternative and complementary investigation approaches, most important is probably the fact that a recently reactivated fault (i.e. a fault that has generated an event in instrumental or historical times, say the last decades or few centuries) is unlikely to be reactivated again in the near future at least in the Aegean region where slip-rates are relatively low and recurrence intervals relatively long. In contrast, tectonic structures which can be geologically recognised as active (especially without instrumentally or even historically documented activity) might be mature enough to rupture in the next future as suggested, for example, for Northern Thessaly (Caputo, 1995). For the finalities of any serious SHA estimate, the degree of maturity of an active fault in the frame of its seismic cycle would be certainly the most crucial aspect. A classic example for Greece would be the 1995 Kozani earthquake that occurred in Western Macedonia, which was earlier considered as a typical 'aseismic' or 'low seismicity' region (Voidomatis, 1989; Papazachos, 1990), exactly due to the lack of seismicity.

In order to better examine this issue and to show the importance of geological data for SHA analyses, in this paper we describe, discuss and compare – deliberately in a separate way – the seismotectonic information that can be obtained from the analysis of *single-event effects* with respect to that obtained from *cumulative effects* of multiple coseismic reactivations. The distinction between the two types of *sources of information* is not just a terminological matter but mainly a methodological one implying that the investigation tools used in the two cases are generally different (Caputo and Helly, 2008). Indeed, *single-event effects* are inherently associated with the reactivation of a fault that took place mainly in historical and/or instrumental times, for which all observations focus on, and are limited to, the specific coseismic effects and associated features. Accordingly, the commonly applied investigation methods are represented by seismological studies, post-event epicentral area surveys, palaeoseismological trenching (trying to detect the last displacement, e.g. Palyvos et al., 2010), critical analysis of oral and/or written witnesses (Historical Seismology; e.g. Papazachos and Papazachou, 1997), investigations on 'disturbed' artefacts like buildings and settlements (Archaeoseismology; e.g. Stiros and Jones, 1996; Caputo and Helly, 2005; Caputo et al., 2010), geodetic surveys (e.g. Stiros and Drakos, 2000; Resor et al., 2005) and satellite analyses (e.g. Meyer et al., 1996; Kontoes et al., 2000). It is obvious that almost all of these methodological approaches (except the palaeoseismological and archaeoseismological ones) have significant time constraints for their application because, on the one side, most of the investigations rely on technologically sophisticated instruments not available in the past (seismographs, satellite products, etc.) and, on the other hand, surficial evidences (e.g. coseismic ground ruptures) are highly vulnerable to weathering, erosion or anthropogenic modifications and quickly fade away.

Conversely, *cumulative effects* represent all the evidences that derive from multiple and repeated recent fault reactivation(s), say during Middle–Late Pleistocene or Holocene. In this case, investigating methods include several typical geological approaches (morphotectonic surveys, structural mapping, stratigraphic and pedological analyses, palaeoseismological trenching, etc.; Caputo and Helly, 2008), remote sensing analyses of air photos and satellite imageries and several geophysical methods, such as electrical resistivity tomographies, ground penetrating radar, high-resolution seismic profiles, and microearthquake surveys.

From a practical point of view, the major difference between the two approaches is that a historically or instrumentally recorded earthquake

Please cite this article as: Caputo, R., et al., Comparison between *single-event effects* and *cumulative effects* for the purpose of seismic hazard assessment. A review from Greece, Earth-Sci. Rev. (2015), http://dx.doi.org/10.1016/j.earscirev.2015.05.004

generally makes evident the occurrence of a fault, therefore guiding the scientists to investigate a specific seismogenic structure and making specific *single-event effects*-based observations. In contrast, most active faults not associated with recent strong events, need to be firstly recognised in the field and only subsequently be investigated by focusing on the associated *cumulative effects*.

3. Comparison between *single-event effects* and *cumulative effects*

In this chapter we consider four case studies of active faults causative of moderate-to-strong seismic events which affected the Aegean Region in the recent past. For the purpose of this paper, we separately follow the two investigating approaches; that is to say, we firstly examine the seismogenic sources using only *single-event effects*-based tools and exclusively relying on *single-event effects* information, therefore deliberately ignoring any *cumulative effects* information. Secondly, we analyse the same seismogenic structures limiting the observations to the *cumulative effects* as if the major earthquake did not occur (i.e. deliberately ignoring the *single-event effects* and associated information) and consequently applying the specific investigation tools previously mentioned.

The selected four case studies (Fig. 1) are represented by well expressed faults, which have been reactivated by earthquakes in different epochs, therefore allowing also to investigate the variable (in time) quality and degree of uncertainty regarding the seismotectonic information that can be obtained from the analysis of *single-event effects*. In Table 1, the seismotectonic parameters for the considered case studies are listed, giving a synthetic view and allowing a direct comparison and brief analysis of the differences and similarities between the two sets of results as obtained by applying the two methodological approaches. According to the reliability and accuracy of the results, a quality factor is also attributed to each parameter. It varies from A, indicating fully reliable and accurate results, to E, representing poorly documented values generally tentatively inferred from empirical relationships and/or with large uncertainty.

In the following chapter (Section 4. Discussion), similarities and especially differences between the numerical results and associated uncertainties obtained following the two approaches and based on the two different *sources of information* are discussed in order to emphasize advantages and limitations.

3.1. South Corinth Gulf Fault System

The Gulf of Corinth is one of the most tectonically active regions worldwide, showing an intense seismicity both in terms of magnitude and frequency. The gulf corresponds to an asymmetric graben which is likely characterized underneath by a low-angle N-dipping fault (Rigo et al., 1996; Bernard et al., 1997; Exadaktylos et al., 2003; Flotté et al., 2005; Gautier et al., 2006; Sachpazi et al., 2007; Skourtsos and Q14
Kranis, 2009, and many others). The southern side of the gulf close to the northern coast of Peloponnesus is affected by an important composite seismogenic source: the South Corinth Gulf Fault System (*a* in Fig. 1; sometimes referred to in the literature as Egion or Aigion Fault). One of the major individual active structures (ISS) of this complex shear zone is the East Heliki Fault (Fig. 3; Rigo et al., 1996; Le Meur et al., 1997; Sorel, 2000; Chéry, 2001; Flotté and Sorel, 2001; Cianetti et al., 2008), which was re-activated during the December 26, 1861 Valimitika earthquake (Fig. 4). This case study has been selected because it represents the first example for Greece of penecontemporaneous systematic field investigations complete of a detailed ground ruptures map (Fig. 5) and a scientific report of many seismically induced effects (Schmidt, 1867; 1879).

3.1.1. Single-event effects

The 1861 earthquake had a maximum intensity X (MCS) and a macroseismic field suggesting an E(SE)-W(NW) trending fault (Fig. 4). The estimated magnitude is 6.7 (Papazachos and Papazachou, 1997) or 6.6 according to Ambraseys and Jackson (1997) and Papadopoulos (2000). The latter magnitude could be considered the maximum expected event for this seismogenic source, given that it also matches the maximum recorded magnitudes from the broader Corinth Gulf (Papadopoulos, 2000). It should also be noted, however, that the magnitude obtained by inversion of the seismic moment (Aki, 1966) calculat- Q15
ed from the inferred parameters (see Table 1) would be somehow smaller (6.5).

As mentioned above, the 1861 earthquake represents the first case in Greece of systematic field investigations carried out within the epicentral area soon after the event thus providing many descriptions and observations about the coseismic effects, like liquefaction, ground ruptures and damages to buildings (Fig. 5; Schmidt, 1867, 1879). Q16
The ground ruptures are considered the surface expression of the

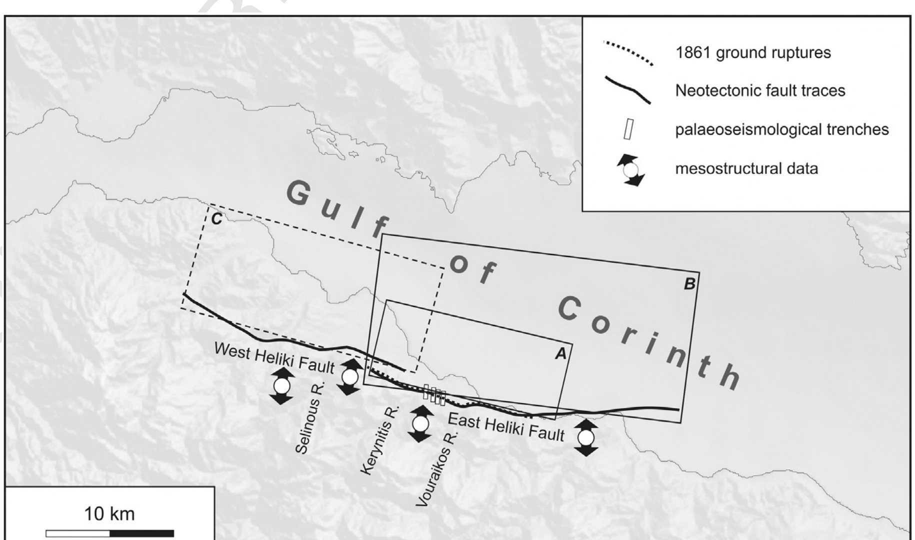

Fig. 3. Map of the South Corinth Gulf Fault System showing the East Heliki seismogenic source obtained from the analysis of *single-event effects* (box *A*) and *cumulative effects* (box *B*). The 1861 ground ruptures (Schmidt, 1867; 1879), the Neotectonic fault traces (Poulimenos and Doutsos, 1996; Roberts and Koukouvelas, 1996; Kokkalas and Koukouvelas, 2005; Koukouvelas et al., 2005), the location of the palaeoseimological trenches (Koukouvelas et al., 2001; Pavlides et al., 2004) and the results of mesostructural analyses (Doutsos and Poulimenos, 1992;
Q1 Stewart, 1996; Micarelli et al., 2003) are also represented. For reference, the West Heliki Fault (box *C*) is also drawn, separated by a right-stepping geometry possibly representing a 'strong' barrier. Seismotectonic parameters of the analysed ISSs (boxes *A* and *B*) are reported in Table 1.

Please cite this article as: Caputo, R., et al., Comparison between *single-event effects* and *cumulative effects* for the purpose of seismic hazard assessment. A review from Greece, Earth-Sci. Rev. (2015), http://dx.doi.org/10.1016/j.earscirev.2015.05.004

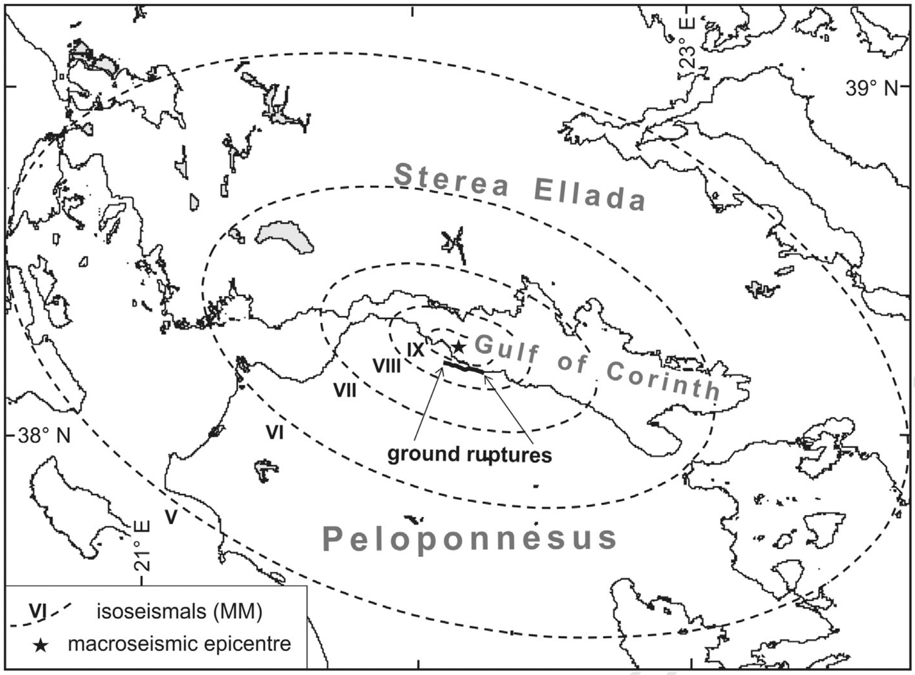

Fig. 4. Isoseismals (MM) and macroseismic epicentre of the 1861 Valimitika earthquake (redrawn from Papazachos et al. (1997).

seismogenic fault (i.e. minimum depth = 0 km) and are aligned in an E(SE)-W(NW) direction, in agreement with the macroseismically inferred fault orientation (assumed strike = 280°).

Accordingly, the surface rupture length was 13–15 km. However, based on magnitude and empirical relationships (Wells and Coppersmith, 1994; Pavlides and Caputo, 2004), this value is

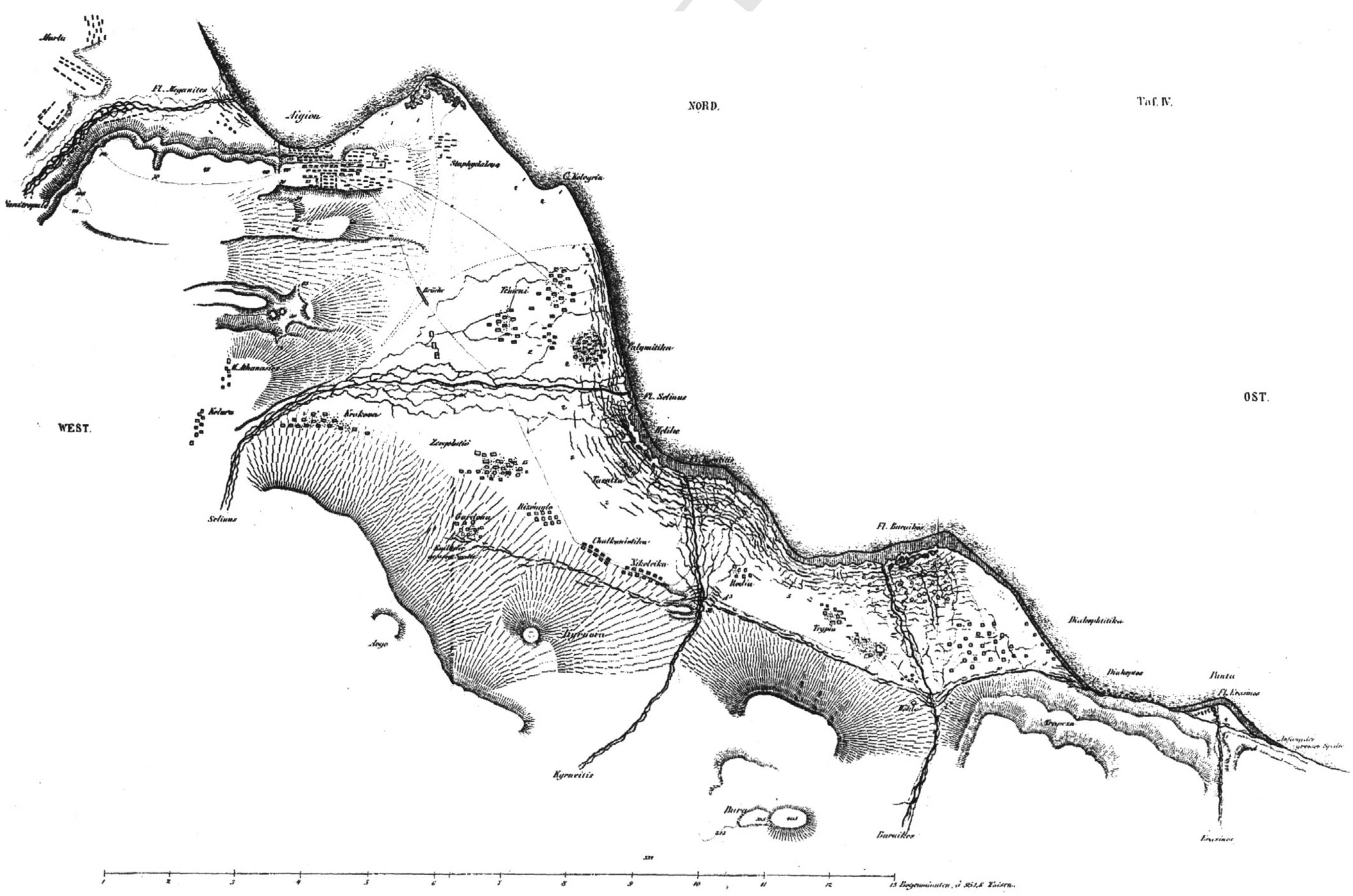

Fig. 5. Reproduction of the original map of Schmidt (1867) relative to the macroseismic area of the 1861 Valimitica earthquake.

certainly underestimated. Accordingly, the fault rupture likely continued offshore for some more kilometres, but no specific information is available from historical sources (assumed value 15 km, see Table 1). The surface displacement was normal (south up, north down) and the maximum observed value was about 1 m. No direct information is available for the dip-angle (assumed value 60° as typical for normal faults), maximum depth and width. The latter parameter could be tentatively inferred from empirical relationships, although the use of different correlated parametres (e.g. width vs magnitude = 16 km; Wells and Coppersmith, 1994; or width vs length = 9 km; Wesnousky, 2008) provides quite different outputs, thus suggesting a large uncertainty for the assumed mean value (12 km) and hence for the maximum depth (10 km).

The 1861 earthquake obviously represents the last event on the East Heliki Fault and therefore the elapsed time is perfectly constrained. Box *A* in Fig. 3 represents the horizontal projection of the individual seismogenic source as obtained from the above values.

3.1.2. Cumulative effects

The trace of the East Heliki Fault has been mapped in detail by several authors (Poulimenos and Doutsos, 1996; Roberts and Koukouvelas, 1996; Koukouvelas et al., 2001, 2005; Kokkalas and Koukouvelas, 2005) and hence the mean strike (277°) is well constrained (Table 1). Morphometric analyses document the linear morphogenic activity Q17 (Caputo, 2005) of the fault (Koukouvelas et al., 2001; Verrios et al., 2004) which has also deflected the flow path of the Kerynitis, Vouraikos and Selinous Rivers (Fig. 3; Pavlides et al., 2004; McNeill et al., 2005) and thus the minimum depth is posed 0 km.

The South Corinth Gulf Fault System (*a* in Fig. 1) consists of two major segments, the East Heliki and West Heliki faults (boxes *B* and *C*, respectively, in Fig. 3), characterized by a right-stepping partially overlapping geometry. Although the issue is still debated in the literature, the stepping distance of about 3 km represents an 'open relay' (e.g. Soliva and Benedicto, 2004) and hence a 'strong segment barrier' (Kato and Hirasawa, 1996) likely halting the coseismic rupture starting from any of the two segments (dePolo et al., 1991; Yeats et al., 1997). Accordingly and focusing only on the East Heliki Fault as the ISS associated with the 1861 earthquake, the geologically and morphotectonically mapped trace on land showing evidences of recent activity is at least 20 km-long (Roberts and Koukouvelas, 1996; Stewart, 1996; Koukouvelas et al., 2001; Micarelli et al., 2003; Verrios et al., 2004). However, the occurrence of uplifted marine terraces and notches on limestone cliffs undoubtedly documents the offshore continuation of the fault (Figs. 6 and Q18 7; Stewart, 1996; Stewart and Vita-Finzi, 1996; McNeill and Collier, 2004), which is further confirmed by seismic profiles (Fig. 8; Stefatos et al., 2002; Lykousis et al., 2007; Bell et al., 2008; Taylor et al., 2011).

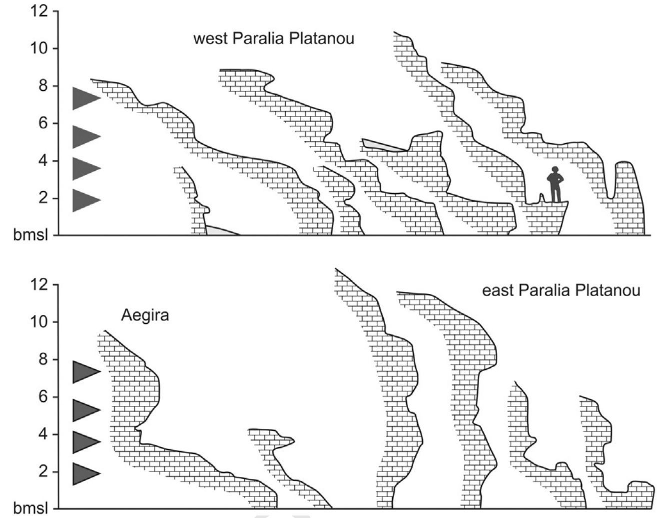

Fig. 7. Coastal profiles at Paralia Platanou and Aegira showing the inferred position (arrow-heads) of prominent erosional levels cut into limestone cliffs (bmsl: biological mean sea level; no vertical exaggeration). Redrawn from Stewart (1996). These *cumulative effects* help in constraining a mean uplift-per-event (viz. slip-per-event), a mean recurrence interval and hence a short-term slip-rate.

Based on the combined information obtained from these *cumulative effects*, the total length of the East Heliki Fault is estimated to be *ca.* 25 km.

Structural analyses on fresh slickensides clearly show an almost pure dip-slip normal kinematics (assumed rake 280°) associated with a N-S-trending tensile stress field (Fig. 3; Doutsos and Poulimenos, 1992; Stewart, 1996; Micarelli et al., 2003).

Microearthquake investigations in the broader area (Rietbrock et al., 1996; Rigo et al., 1996; Gautier et al., 2006; Bourouis and Cornet, 2009), help in constraining the seismogenic layer thickness, the geometry at depth and the possible interaction with a low-angle detachment underlying the Corinth Gulf (Fig. 9). Taking into account the overall geometry and considering a likely mechanical continuity with the low-angle segment, we could estimate some parameters like the maximum depth (*ca.* 10 km), the width (15.5 km) and a mean dip-angle value (40°; assuming a simplified planar fault plane as required for the ISSs of GreDaSS; Fig. 2; see also Basili et al. (2008)).

Slip-per-event has been obtained from several palaeoseismological trenches (Koukouvelas et al., 2001; Pavlides et al., 2001, 2004; Chatzipetros et al., 2005) and ranges from 0.5 to *ca.* 2.0 m (Fig. 10) suggesting a mean value of 0.8 m (Table 1).

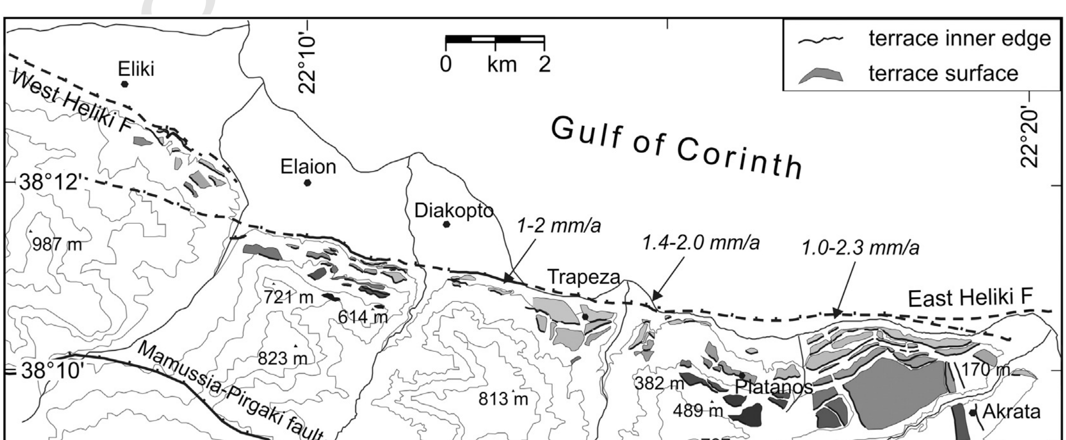

Fig. 6. Map of the marine terraces uplifted in the footwall block of the East Heliki Fault (redrawn from McNeill and Collier (2004)) documenting the recent activity and the cumulative effects along the eastern offshore portion of this seismogenic source. Values in mm/a refer to uplifted Holocene notches and beaches.

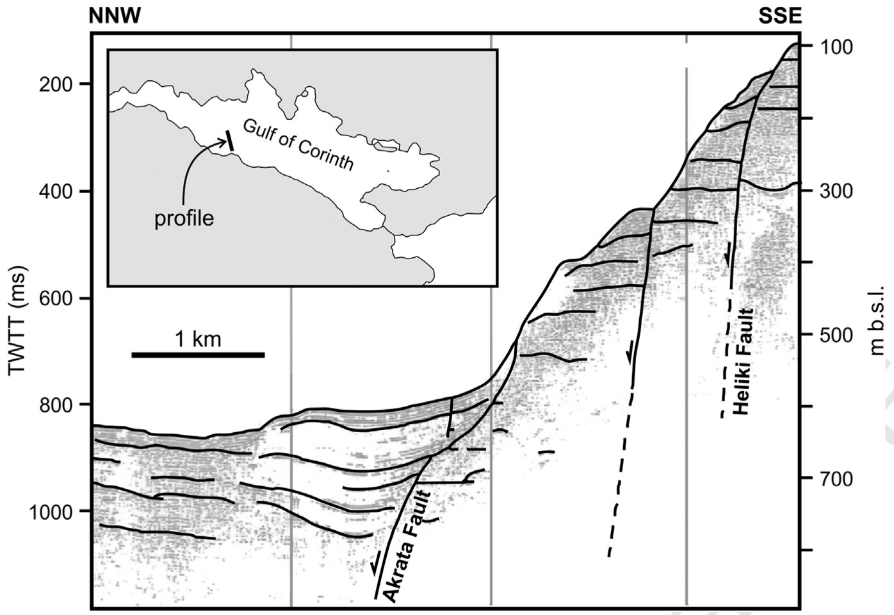

Fig. 8. Interpreted air-gun profile carried out offshore the Akrata village showing that the southern limit of the Corinth Gulf (see inset map for location) is actually controlled by the East Heliki Fault (modified from Stefatos et al. (2002)); these *cumulative effects* document the eastern offshore continuation of the ISS.

The determination of the slip-rate is based on different investigation methods that provide data for both short- and long-term values. For example, direct measurements, like palaeoseismological trenches or seismic reflection profiles (Koukouvelas et al., 2005; Chatzipetros et al., Q19 2005; McNeill et al., 2005; Bell et al., 2009) suggest values varying between 0.3 and *ca.* 5 mm/a. On the other hand, indirect inferences, like using the coastal uplift or GPS extension rates (De Martini et al., 2004; McNeill and Collier, 2004; Pirazzoli et al., 2004) generally provide higher values (3–11 mm/a) that are commonly explained by the authors due to aseismic 'creep' and/or displacement partitioned on multiple subparallel faults. Palaeoseismological investigations suggest that during the Holocene, seismic reactivations were clustered in short periods of higher slip-rate separated by long periods of quiescence. Moreover, both trenches and raised marine notches document higher values during the Holocene with respect to the Late Pleistocene, confirming a variable seismotectonic behaviour and a recently increased slip-rate (e.g. Stewart, 1996; Koukouvelas et al., 2005). Based on the critical analysis of the above information, we assume 0.5–2.0 mm/a as a tentative range of values for the slip-rate, while considering also geomorphological results (Mouyiaris et al., Q20 1992; Stewart, 1996) a possible recurrence interval between 200 and 1600 years could be inferred.

For the purpose of this paper devoted to test the reliability of the two different *sources of information*, we hypothetically assume to ignore the exact date of the 1861 event. Notwithstanding, palaeoseismological investigations somehow contribute to constrain the timing of the last event (<700 years BP) and therewith the elapsed time (<600 years).

Using the obtained length, width and slip-per-event and assuming a realistic value for rigidity, a maximum expected magnitude of 6.6 (M_w) can be finally estimated by means of the seismic moment (Aki, 1966). Q21

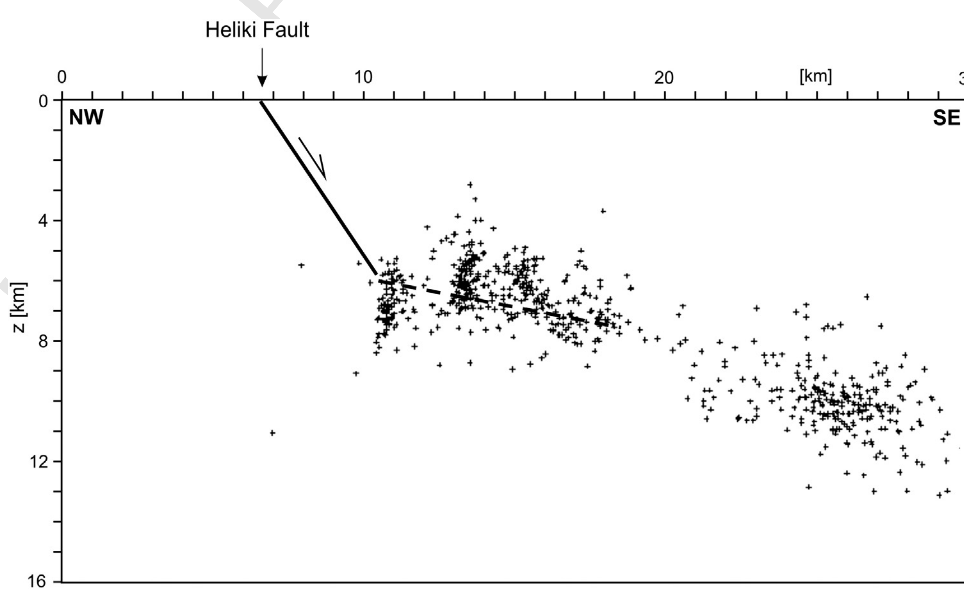

Fig. 9. Hypocentral distribution of the microseismic activity across the western sector of the Eliki Fault (Bourouis and Cornet, 2009) constraining the geometry of the structure, its connection with a low-angle detachment (dashed line), the maximum seismogenic depth and hence the fault width.

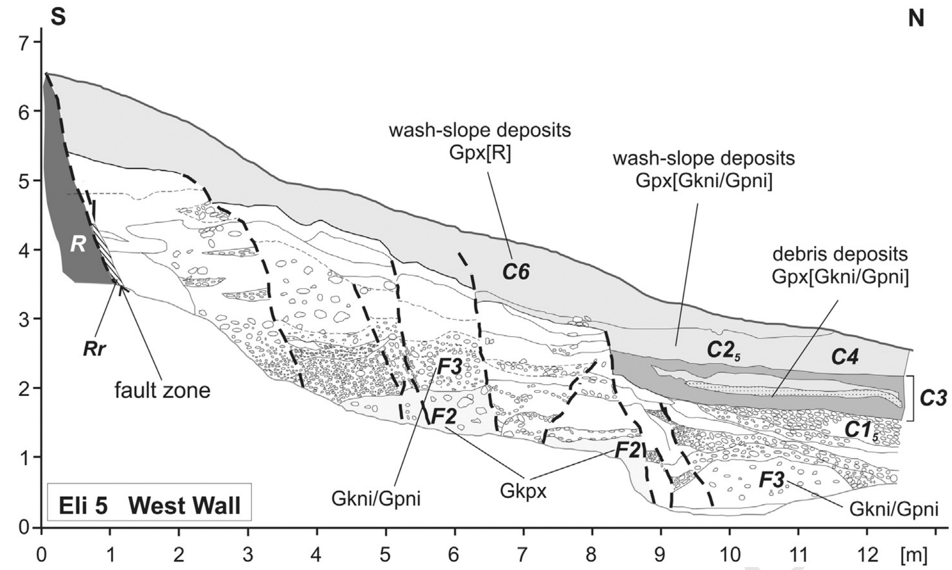

Fig. 10. Example of palaeoseismological trench across the Eliki Fault trace providing information on the slip-per-event, the recurrence interval and hence the (short-term) slip-rate (modified from Pavlides et al. (2004)). Alphabetic codes refer to the Nelson's (1992) classification for colluvial deposits, while *Fn* and *Cn* are stratigraphic units codes referred to in the original paper.

3.2. Domokos Fault System

The second case study is represented by a major fault zone affecting southwest Thessaly and referred to as Domokos Fault System (*b* in Fig. 1; Caputo, 1995). This structure runs along the boundary between the Karditsa Plain, to the NE, and the Pindos mountain range, to the SW (Fig. 11). The geological and tectonic complexity of the structure is certainly due to its poly-phased evolution and the present-day seismogenic source likely developed by exploiting several inherited sliding surfaces represented by NW-SE trending Oligocene–Miocene thrust planes, mainly inverted during the Pliocene (-Early Pleistocene) NE-SW extensional post-collisional collapse and further reactivated in the frame of the still active N-S crustal stretching (Caputo and Pavlides, 1993). As a consequence, in Middle–Late Quaternary these structures started branching and linking with newly generated, E-W trending, fault segments. The Domokos Fault System was largely reactivated during the April 30, 1954 Sophades earthquake (Fig. 12).

3.2.1. Single-event effects

Although the Sophades earthquake occurred during the instrumental period, at that time the European and especially the Greek seismographic networks were not particularly developed and hence the available seismological information is relatively poor. According to the recordings of the National Observatory of Athens (after Papastamatiou and Mouyiaris (1986)), the originally reported magnitude was $M_s = 7.0$, while a revised surface waves magnitude of 6.7 was proposed by Ambraseys and Jackson (1990). The latter value has been considered as a more reliable maximum expected magnitude for this ISS (Table 1). As

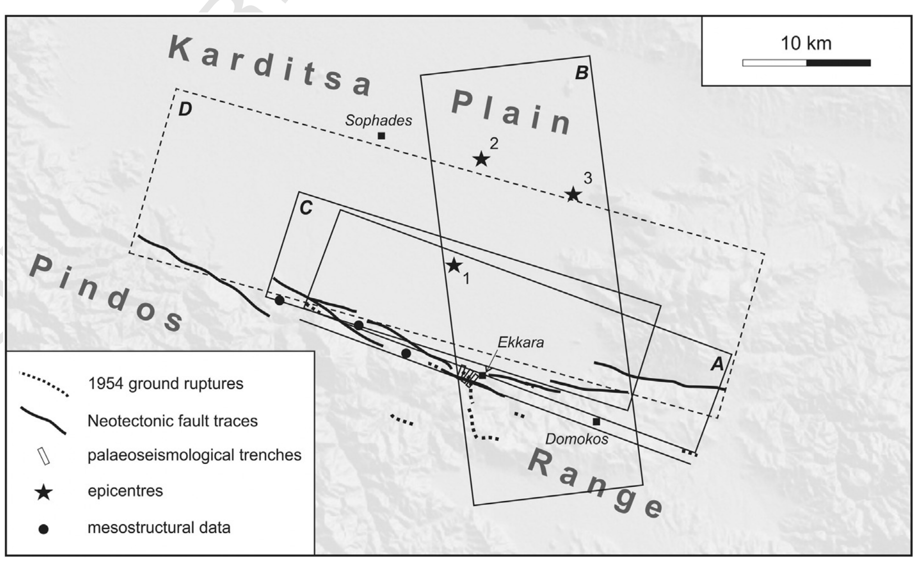

Fig. 11. Map of the Domokos Fault System, Southern Thessaly, showing the seismogenic sources obtained from the analysis of *single-event effects* (two alternative solutions: boxes *A* and *B*) and of *cumulative effects* (box *C*). The 1954 ground ruptures (Papastamatiou and Mouyaris, 1986), the Neotectonic fault traces (Caputo, 1990; Valkaniotis, 2005; Palyvos and Pavlopoulos, 2008), the location of the palaeoseismological trenches (Palyvos et al., 2010), the sites of mesostructural analysis (Caputo, 1990; Caputo and Pavlides, 1993) and the proposed epicentres (1 = McKenzie, 1972; 2 = National Observatory of Athens; 3 = Papazachos et al., 1982) are also represented together with a hypothetical, but discarded, alternative 'geological' solution (box *D*; see text for discussion). Seismotectonic parameters of the analysed ISSs (boxes *A*, *B* and *C*) are reported in Table 1.

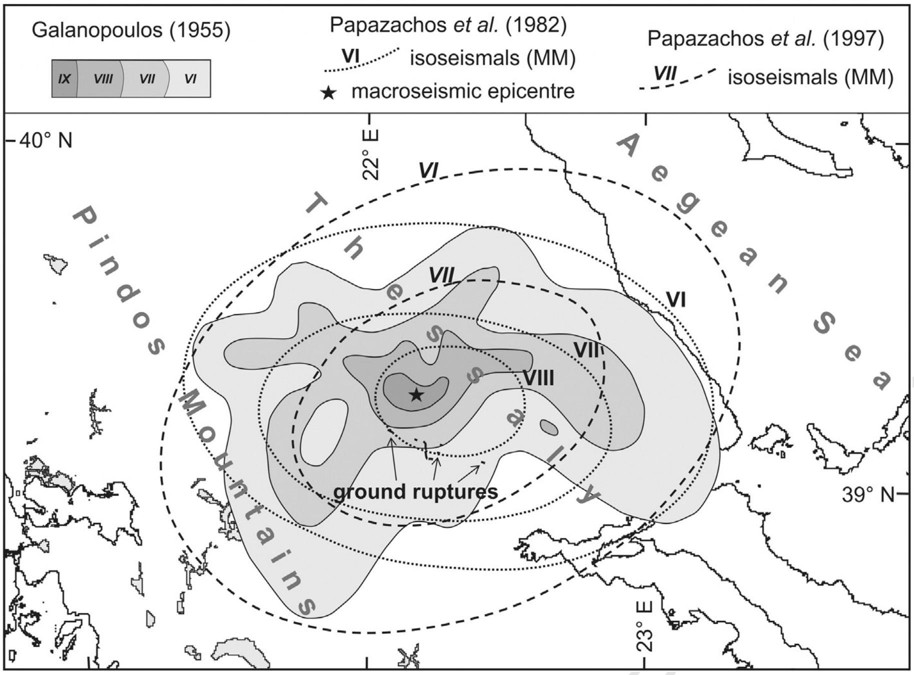

Q2 **Fig. 12.** Isoseismals and macroseismic epicentre of the 1954 Sophades earthquake from Galanopoulos (1955; in Galanopoulos (1959); Papazachos et al. (1982) and Papazachos et al. (1997).

concerns the geographical location of the source, different epicentres have been proposed, all located well north the morphological boundary between mountain range and alluvial plain (Fig. 11).

The macroseismic field has been firstly reconstructed by Galanopoulos (1955, in Galanopoulos, 1959) and revised by Papazachos et al. (1982, 1997); (Fig. 12). Notwithstanding the large number of intensity points considered during the revisions (152), the isoseismal patterns largely differ both in orientation and shape (Fig. 12), thus suggesting the large uncertainty intrinsic in the proposed maps and hence in the possible location and orientation of the causative fault.

The first field observations of the coseismic ground ruptures took place five days after the main shock (see notes by Yannis Papastamatiou in Papastamatiou and Mouyiaris (1986)), describing a major NNW-SSE-trending fracture only few kilometres-long (7–8 km; Fig. 11). This length is certainly not appropriate for a strong (assumed magnitude 6.7) upper-crust normal fault earthquake that should be associated with an emergent rupture plane (i.e. ‘linear morphogenic earthquake’; Q22 Caputo, 2005) more than 20 km-long (Pavlides and Caputo, 2004). At this regard and speculating on some isolated ground fractures observed almost 15 km WNW of Ekkara and 6 km ESE of Domokos (Fig. 11), and tentatively assuming a possible blind (or unmapped?) continuity of the coseismic rupture, the total surface length would be *ca.* 23 km.

Maximum observed dislocation was 90 cm, characterized by a large heave and a left-lateral strike-slip component of relative motion, causing the subsidence of the northeastern block (Fig. 13). Papastamatiou and Mouyiaris (1986) hesitantly associate these surface fractures with the seismogenic fault, therefore suggesting a minimum depth of the ISS (i.e. top of the fault) greater than 0 km (we conventionally assigned 1 km).

Using length-to-width empirical relationships (Wesnousky, 2008; Leonard, 2010) the width is in the range 14–15 km, while taking into account the preferred magnitude and length (Table 1) and assuming a reasonable value for rigidity and average slip (say, 1 m for a M6.7 earthquake), a width of 17.5 km is obtained. All these values are in contrast with the proposed epicentral locations as far as the horizontal projection of any of these fault planes would not include them (Fig. 11). If we i) disregard this seismological information (i.e. epicentral locations), ii) consider a preferred width value of 16 km and iii) assume a dip angle of 60° typical for normal faults, the maximum depth could thus be estimated (15 km). Accordingly, the proposed ISS is represented by box *A* in Fig. 11 (inferred strike 295°).

The proposed seismogenic source could justify the Galanopoulos Q23 (1955) and Papazachos et al. (1982) macroseismic fields, but not the

Fig. 13. View of the 1954 co-seismic ESE-WNW-trending ground rupture cutting the alluvial deposits few hundred metres NW of Kato Agoriani village (actually named Ekkara; photo from Papastamatiou and Mouyaris (1986)). See Fig. 11 for location.

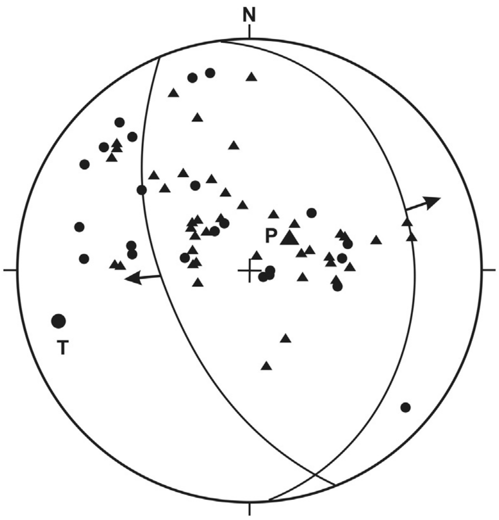

Fig. 14. The focal mechanism proposed by McKenzie (1972) for the 1954 Sophades earthquake based on first motion polarities from short period seismic records suggesting a NE-dipping nodal plane oriented NNW-SSE.

most recent revision (Papazachos et al., 1997) and above all it is not in agreement with the focal mechanism of the main shock (McKenzie, 1972; Fig. 14). Indeed, the preferred fault plane solution based on first motion polarities from short period seismic records indicates a NNW-SSE-trending nodal plane (assumed strike, dip and rake of 353°, 29° and 300°, respectively). Following the above approach procedure based on existing empirical relationships, it could be also possible to tentatively constrain the geometrical parameters (Table 1). This alternative solution (box *B* in Fig. 11) would be in better agreement with the major ground ruptures observed during the post-seismic field survey (Papastamatiou and Mouyiaris, 1986) and bearing an oblique-slip kinematics, but it would be conflicting with the epicentral location and especially the inferred maximum depth is likely too shallow for a strong earthquake.

In conclusion, information provided by *single-event effects* are somehow contradicting because some field observations and the macroseismic field suggest an ESE-WNW trending almost blind plane (box *A* in Fig. 11), while the focal mechanism and the major ground ruptures indicate a NNW-SSE-trending oblique-slip (normal and left-lateral) fault (box *B* in Fig. 11). By default, *single-event effects* do not provide information regarding the recurrence interval nor the slip-rate.

3.2.2. Cumulative effects

Based on detailed geological and morphotectonic mapping (Caputo, 1990, 1995; Caputo and Pavlides, 1993; Valkaniotis, 2005), a geometrically complex fault zone with clear evidences of Quaternary activity has been recognised. The fault strike is almost E-W, in the eastern sector, and WNW-ESE, in the western sector. The cumulative length of the whole fault zone bearing clear evidence of neotectonic activity (Caputo et al., 2008) is *ca.* 50 km (box *D* in Fig. 11). Accordingly, the minimum depth is assumed = 0 km.

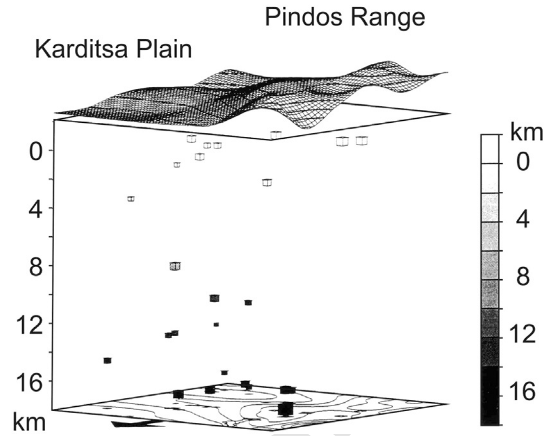

Fig. 16. Depth distribution of the microseismicity in southern Thessaly showing maximum values at *ca.* 15 km. The arrow on the bottom indicates the north direction. Modified from Kementzetzidou (1996).

The structure is composite, probably still evolving (i.e. in a phase of alternating growing and connecting segments; Schultz and Fossen, Q24 2002; Kim and Sanderson, 2005) and characterized by several minor Q25 segments on the way to be interconnected by the coalescence and reactivation of inherited sliding planes (Figs. 11 and 15). The different segment boundaries show a left-stepping geometry and sometimes a partial overlap; these two parameters likely determine the occurrence of a hard- versus a soft-boundary (e.g. Soliva and Benedicto, 2004, and references therein). In particular, the two central segments (Leondari and Velessiotes; Fig. 15) could likely behave as a unique seismogenic source due to the large overlapping geometry and an offset of less than 1 km (i.e. 'fully breached relays'; Soliva and Benedicto, 2004) potentially not sufficient for arresting a coseismic rupture (Yeats et al., 1997). Accordingly, the total length of the considered ISS is *ca.* 30 km, while the strike is 285° (box *C* in Fig. 11).

Maximum depth (~15 km) is constrained according to microseismicity distribution (Fig. 16; Kementzetzidou, 1996; Hatzfeld et al., 1999) and geological–geophysical considerations on the local crustal thickness, crustal rheology and the brittle–ductile transition depth (Sboras, 2012). Assuming a typical dip-angle for normal faults (60°), the width could be also estimated (*ca.* 17 km) based on trivial trigonometry providing a value in good agreement with empirical relationships between geometric parameters (16 and 17 km; from Wesnouski, Q26 2008, and Leonard, 2010, respectively).

Palaeoseismological investigations recently carried out by Palyvos et al. (2010) provide evidence that part of the ground ruptures observed after the 1954 Sophades earthquake near Ekkara village were likely

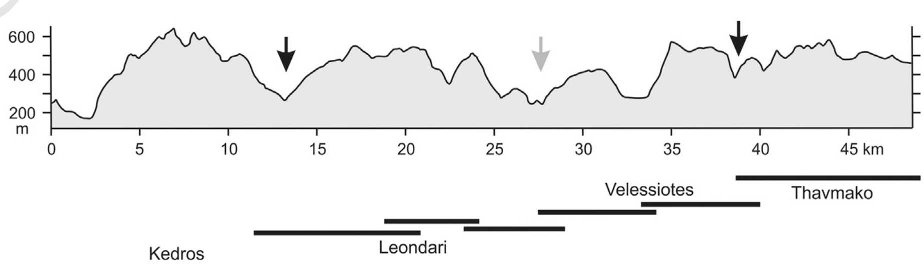

Fig. 15. Distribution of the cumulative displacement measured along strike of the Domokos Fault System showing the occurrence of four major segments separated by hard- and soft-boundaries (black and grey arrows, respectively). Bars below the graph indicate location of the segments and schematically show the relative overlapping and overstepping geometry. Modified from Valkaniotis (2005).

Please cite this article as: Caputo, R., et al., Comparison between *single-event effects* and *cumulative effects* for the purpose of seismic hazard assessment. A review from Greece, Earth-Sci. Rev. (2015), http://dx.doi.org/10.1016/j.earscirev.2015.05.004

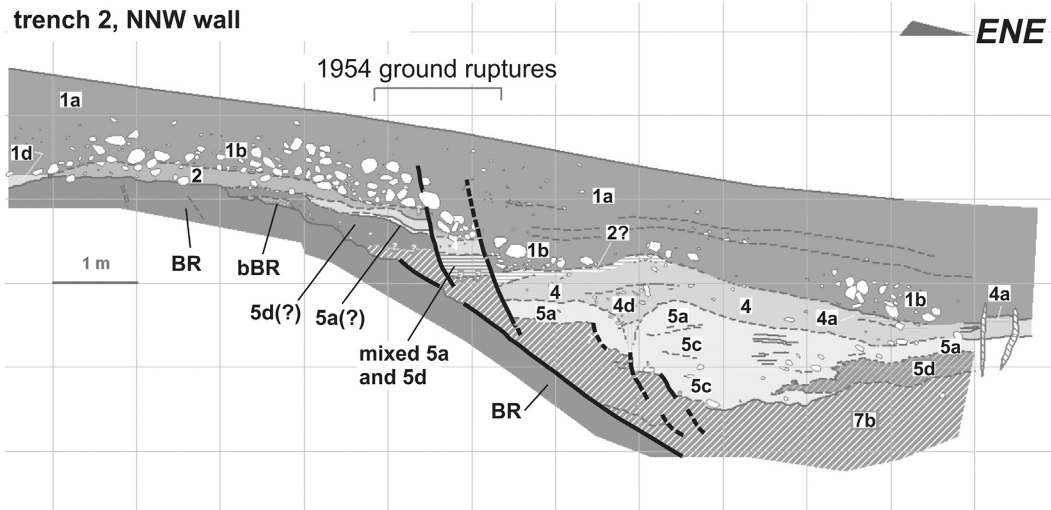

Q3 **Fig. 17.** Log of a palaeoseismological trench excavated across the 1954 ground ruptures near Ekkara showing the occurrence of pre-1954 linear morphogenic earthquakes (Caputo, 2005). Modified from Palyvos et al. (2010). Numbers/letters indicate different stratigraphic units referred to in the original paper.

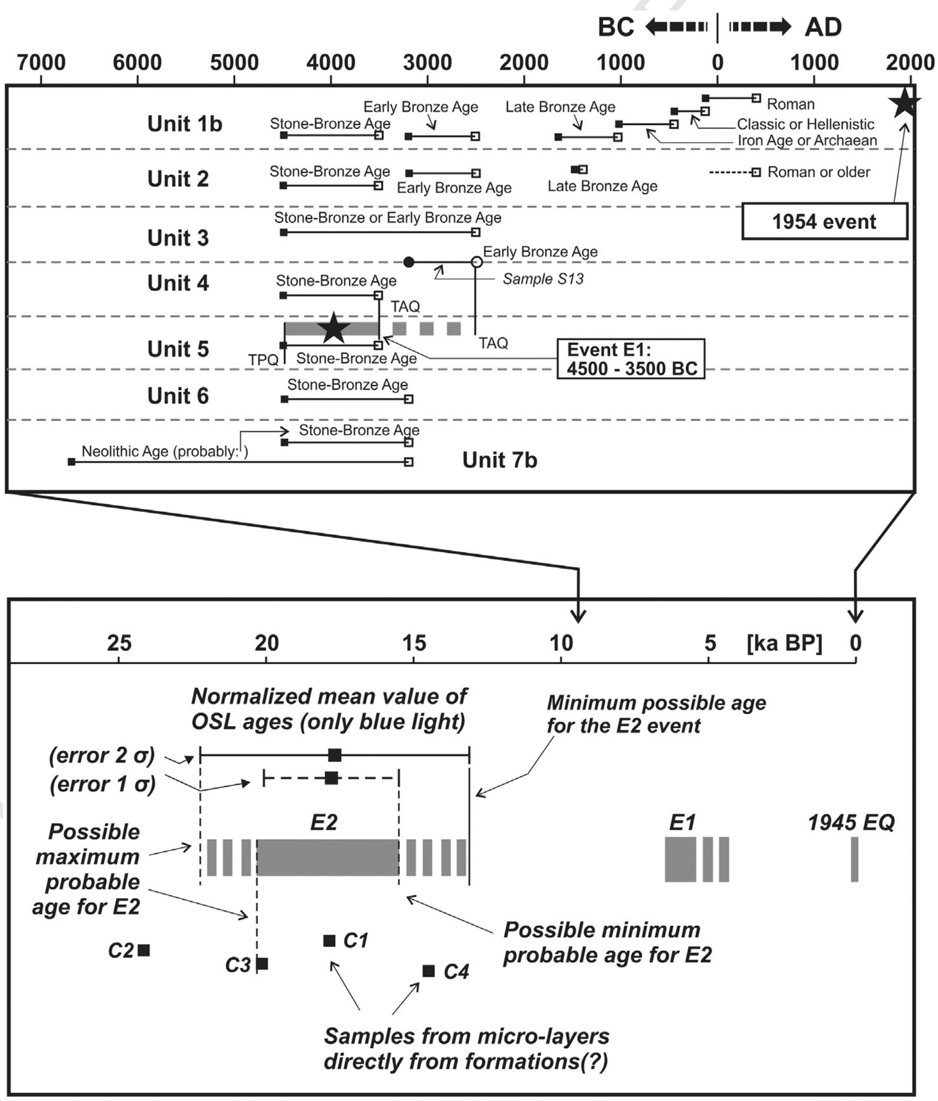

Fig. 18. Inferred timing of the pre-1954 event as obtained from a palaeoseismological investigation and enabling to estimate a mean recurrence interval. Modified from Palyvos and Pavlopoulos (2008).

Please cite this article as: Caputo, R., et al., Comparison between *single-event effects* and *cumulative effects* for the purpose of seismic hazard assessment. A review from Greece, Earth-Sci. Rev. (2015), http://dx.doi.org/10.1016/j.earscirev.2015.05.004

connected with the seismogenic surface (Fig. 11). They also clearly document the occurrence of at least three linear morphogenic events, and possibly four, during the last 17–20 ka (Fig. 17). The measured slip-per-event ranges between 1 and 2 m, but considering their hypothesis of additional events, the preferred value is about 1 m. The calculated slip-rate is 0.3–1.0 mm/a, while the suggested recurrence interval is >3.2 ka (Fig. 18; Palyvos et al., 2010).

For the purpose of this paper, if we suppose to ignore the date of the last event (e.g. 1954), the palaeoseismological investigations would have provided only a weak chronological constraint for the last event (post 500 AD) and hence of the elapsed time (<1.5 ka BP), within the uncertainties of the applied archaeological dating technique (Palyvos et al., 2010), but well below the suggested recurrence interval.

Systematic mesostructural analyses within the broader area (Caputo, 1990; Caputo and Pavlides, 1993) document for the (Middle–Late) Quaternary a prevailing dip-slip kinematics with a slight left-lateral component associated with a *ca.* N-S direction of extension (Fig. 19a–c). This is also confirmed by observations within the palaeoseismological trenches (Fig. 19d). The assumed rake is 285°.

Finally, the above parameters as obtained from the analysis of *cumulative effects* allow estimating the maximum expected magnitude ($M_w = 6.8$), as a worst-case scenario assuming that the two central segments of the Domokos Fault (Leondari and Velessiotes), for a total length of 30 km, are reactivated (box *C* in Fig. 11).

3.3. Mygdonia Fault System

The southern border of the Mygdonia Basin is characterized by an important fault zone mainly striking in a rough E-W direction (*c* in Fig. 1). The fault system crosses obliquely the Cimmerian and Alpine orogenic features though it locally follows some NW-SE-trending inherited discontinuity (Mountrakis et al., 1983; Pavlides and Kilias, 1987; Fig. 20). As a third case study, we focus on a major segment of this fault system, the Gerakarou Fault, which has been re-activated by the June 20, 1978 Stivos earthquake, heavily affecting the city of Thessaloniki, the second largest metropolitan urban area of Greece (Fig. 21).

3.3.1. Single-event effects

The epicentral area of the Stivos earthquake is located in the centre of the Mygdonia Basin, between the Lakes of Koronia and Volvi, about 30 km E(NE) of Thessaloniki (Figs. 20 and 21). The estimated seismic moment ranges between $2.7 \cdot 10^{18}$ and $8.7 \cdot 10^{18}$ (corresponding to $M_w = 6.2$–6.6) and differences generally depend on the applied method, like P-wave spectrum analysis, trial-and-error waveform modelling, generalized inversion of teleseismic P and Sh waves or CMT (Kulhánek and Meyer, 1979; Barker and Langston, 1981; Soufleris and Stewart, 1981). A mean conservative value of 6.6 could be considered the maximum expected magnitude (Table 1).

Several focal mechanisms of the main shock have been proposed by different authors (Fig. 21; Barker and Langston, 1981; Soufleris and

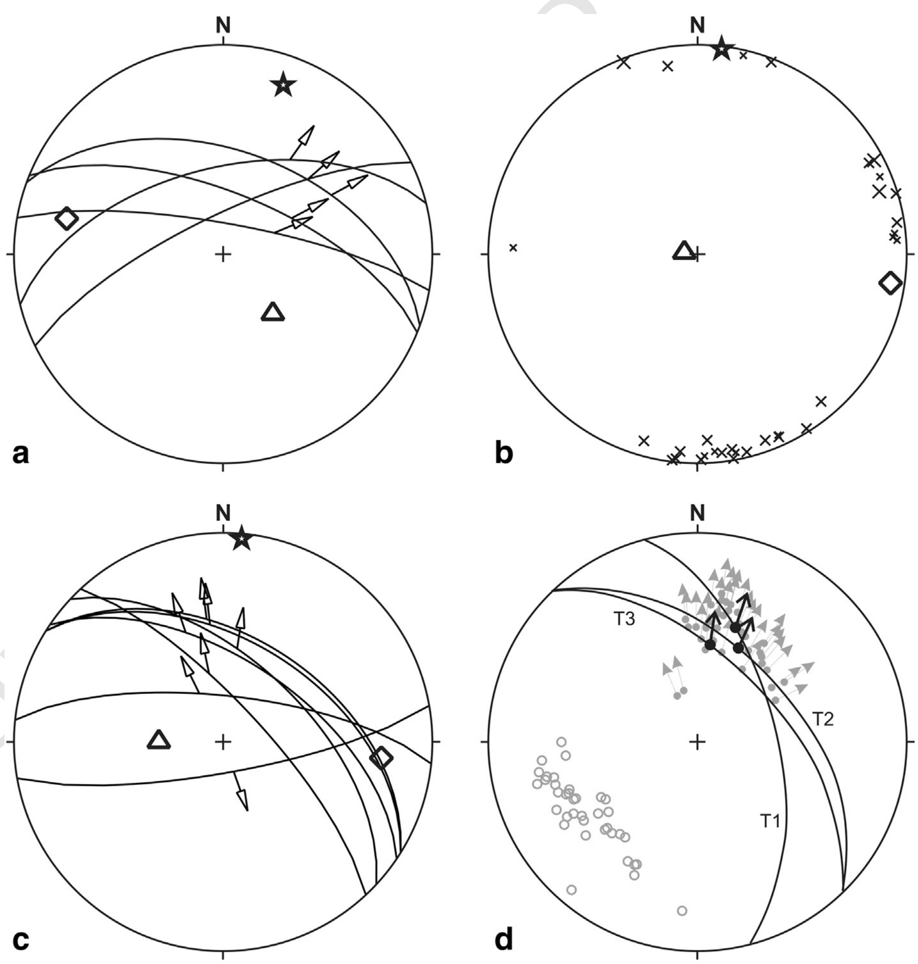

Fig. 19. Results of quantitative mesostructural analyses based on faults ((a) and (c)) and extensional joints (b) collected in the broader area of the Domokos Fault System and attributed to the Middle Pleistocene–Present extensional phase (from Caputo (1990)). The principal stress axes obtained from numerical inversions (Caputo and Pavlides, 1993) are also reported (triangles: σ_1; rhombs: σ_2; stars: σ_3). d) Slickensides measured in the palaeoseismological trenches excavated by Palyvos et al. (2010), where black curves with arrows indicate the average striated plane observed in each trench (T1, T2 and T3); grey arrows and small circles represent all measured slip-vectors and poles to plane, respectively (redrawn from Palyvos and Pavlopoulos (2008)).

Please cite this article as: Caputo, R., et al., Comparison between *single-event effects* and *cumulative effects* for the purpose of seismic hazard assessment. A review from Greece, Earth-Sci. Rev. (2015), http://dx.doi.org/10.1016/j.earscirev.2015.05.004

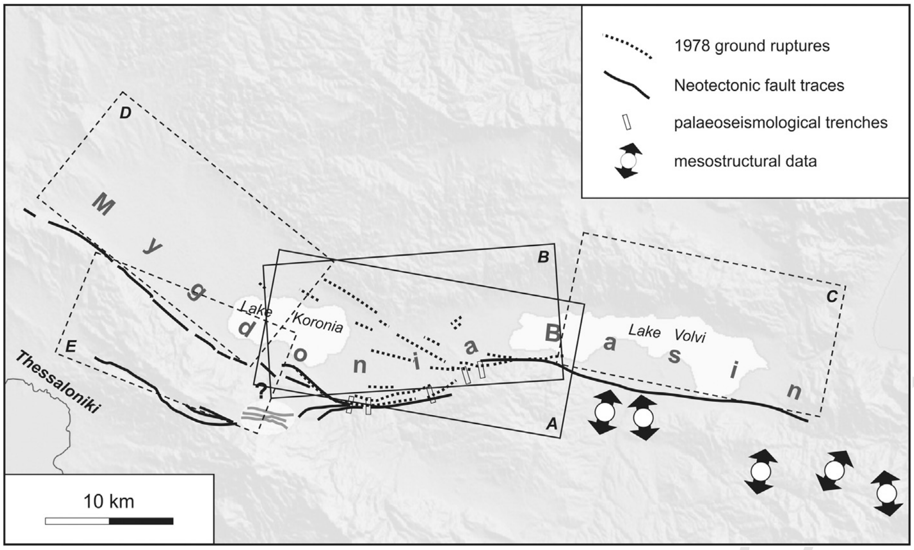

Fig. 20. Map of the Mygdonia Fault System, Central Macedonia, showing the Gerakarou seismogenic source obtained from the analysis of *single-event effects* (box *A*) and *cumulative effects* (box *B*). The Neotectonic fault traces, the 1978 ground ruptures, the location of the palaeoseimological trenches and the results of mesostructural analyses are also represented. The other major segments of the fault system are: Lagadhas Fault (box *D*), Apollonia Fault (box *C*) and Asvestochori Fault (box *E*). See text for discussion and full reference list. Seismotectonic parameters of the analysed ISSs (boxes *A* and *B*) are reported in Table 1.

Stewart, 1981; Dziewonski et al., 1987; Vannucci and Gasperini, 2003, 2004). They substantially agree showing roughly E(SE)-W(NW)-striking nodal planes (273°–289°), dipping between 43° and 55°, with a prevailing dip-slip kinematics and some left-lateral component (rake 272°–300°). According to the occurrence of coseismic ground ruptures, the preferred seismic plane is the N-dipping one. The assumed mean values are reported in Table 1.

Proposed hypocentral depths are 8 km (Soufleris and Stewart, 1981), 10 km (Dziewonski et al., 1987), 11 ± 1 km (Barker and Langston, 1981), 12–15 km (according to NEIS and CSEM agencies, see Carver and Bollinger (1981)) and 16 ± 5 km (Kulhánek and Meyer, 1979). Also the aftershock distribution, was monitored soon after the major event by a local temporary network (Fig. 22; Carver and Bollinger, 1981; Soufleris et al., 1982). However, the results published in the literature are not sufficient for better defining shape and dimensions at depth of the fault surface. This was probably due to the odd geometry and density of the seismographic network, the technological limitations of the used instrumentation, or the velocity model applied for the inversion of the data. In conclusion, a preferred value for the maximum depth of the seismogenic source could be 12 km. Considering the case of an emergent fault (i.e. minimum depth = 0 km); as suggested by the ground ruptures, the assumed maximum depth and the dip-angle of the preferred nodal plane, a fault width of 16 km could be calculated (box *A* in Fig. 20).

Fault dimensions have been constrained based on the inversion of P and Sh waveforms (Roumelioti et al., 2007) suggesting a *ca.* 25 km-long

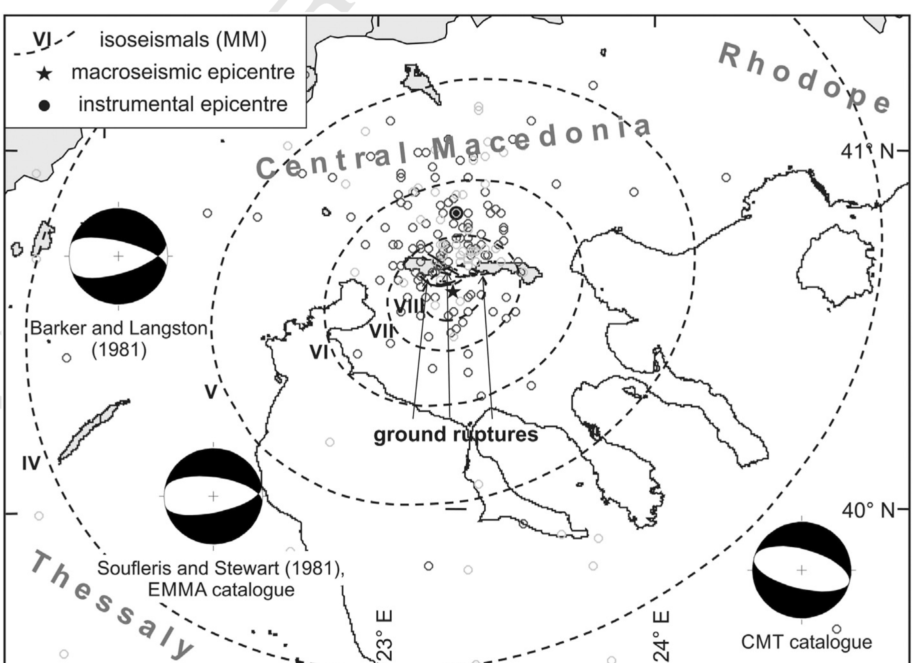

Fig. 21. a) Isoseismal curves, macroseismic and instrumental epicentres of the 1978 Stivos earthquake. Foreshocks and aftershocks are also represented as light and dark grey cirlces, respectively. The location of the ground ruptures and some focal mechanisms of the main shock are also represented. See text for discussion and full reference list.

Please cite this article as: Caputo, R., et al., Comparison between *single-event effects* and *cumulative effects* for the purpose of seismic hazard assessment. A review from Greece, Earth-Sci. Rev. (2015), http://dx.doi.org/10.1016/j.earscirev.2015.05.004

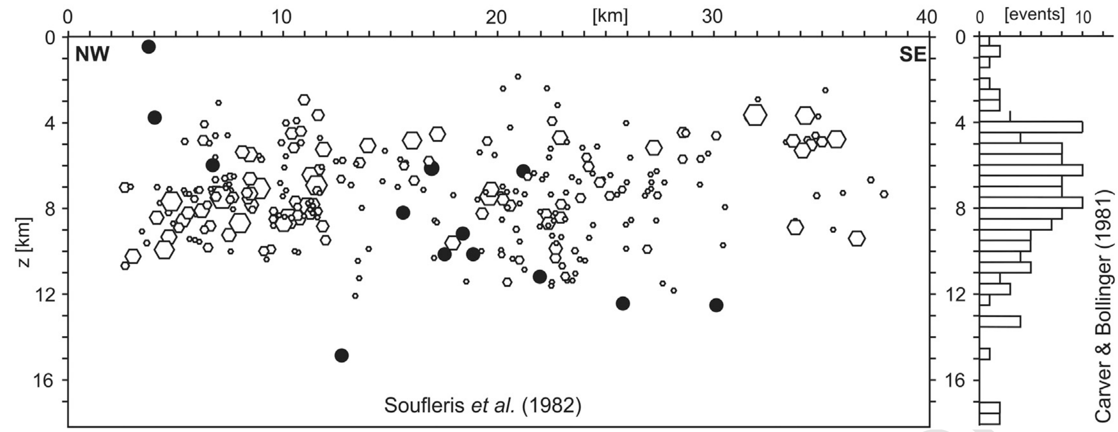

Fig. 22. Depth distribution of the 1978 seismic sequence (left: redrawn from Soufleris et al. (1982); right: histogram data from Carver and Bollinger (1981)) showing a maximum seismogenic depth of 12 km with just few exceptions.

rupture plane and confirming the above-mentioned preferred width value (Fig. 23). The coseismic ground ruptures followed three major alignments (Fig. 20) characterized by different strike and kinematics but showing a mechanical consistency and an overall NNW-SSE lengthening direction (Fig. 24; Mercier et al., 1979, 1983; Papazachos et al., 1979). The most important set of fractures, trending ENE-WSW, runs parallel to the southern margin of the basin for *ca.* 23 km and likely corresponds to the surface expression of the causative fault. A mean value (24 km) between seismological inferences and field observations has Q27 been assumed. It is worth noting that a blind faulting model has been proposed (Stiros and Drakos, 2000) on the assumption that the observed ground ruptures represent secondary coseismic effects.

The average and maximum displacements observed in the field are 8–10 cm and 25 cm, respectively (Fig. 25; Pavlides and Caputo, 2004) in agreement with seismological data (Fig. 23). The mean displacement for the whole fault plane estimated on the basis of seismological data varies from 0.25 to 0.95 m (Kulhánek and Meyer, 1979; Soufleris and Q28 Stewart, 1981; Soufleris et al., 1982; Soufleris and King, 1983; Roumelioti et al., 2007), while the geodetic models suggest a mean coseismic motion of 0.45 or 0.57 m (Stiros and Drakos, 2000). Based on the above, a mean value of 0.5 m has been assumed (Table 1).

3.3.2. Cumulative effects

Geological and morphotectonic mapping of the Mygdonia Fault System clearly documents the occurrence of recent fault scarps (i.e. minimum depth = 0 km) and associated faults running along the southern margin of the plain (Fig. 20; Kockel and Mollat, 1977; Mercier et al., 1979; Mountrakis et al., 1996; Chatzipetros, 1998; Tranos et al., 2003). The structure is composed of few major segments trending between E(NE)-W(SW) and (W)NW-(E)SE. The central sector of the fault system is represented by the Gerakarou Fault (box *B* in Fig. 20), which is delimited to the east by an angular boundary connecting with the Apollonia Fault (box *C* in Fig. 20), while showing to the west either an angular boundary with the (W)NW-(E)SE trending Langadha Fault (box *D* in Fig. 20) and possibly a left-stepping geometry with the Asvestochori Fault (box *E* in Fig. 20). With the latter structure, Tranos et al. (2003) suggest the occurrence of a possible linkage zone (question mark in Fig. 20). Assuming hard segment boundaries at both sides, the Neotectonic fault length (Caputo et al., 2008) of the Gerakarou Fault is therefore *ca.* 23 km and its mean strike 265° (Table 1).

Mesostructural analyses within the seismogenic volume document a Quaternary NNW-SSE-trending extensional field (Fig. 26; Mercier et al., 1983; Pavlides and Kilias, 1987) from which a mean rake of 280° could be inferred.

Microearthquake investigations (Hatzfeld et al., 1986/87; Tranos et al., 2003; Galanis et al., 2004; Paradisopoulou et al., 2006) constrain the seismogenic layer thickness down to a maximum depth of *ca.* 15 km (Fig. 27), also suggesting a listric fault surface characterized by a dip-angle varying between 70° (upper 8 km) and 46° (deeper

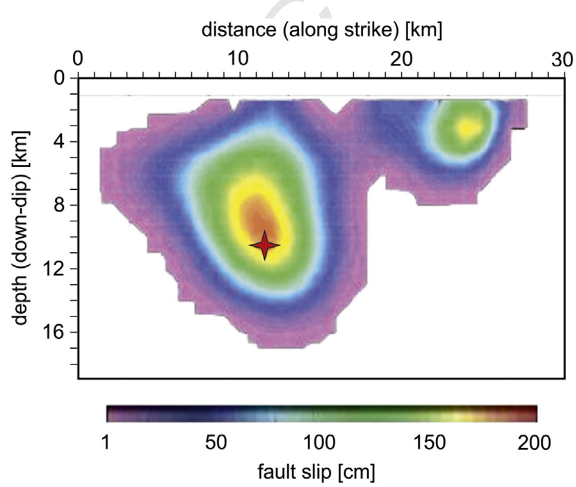

Fig. 23. Slip distribution on the fault plane as computed from the joint inversion of P and S waveforms and geodetic data. Modified from Roumelioti et al. (2007).

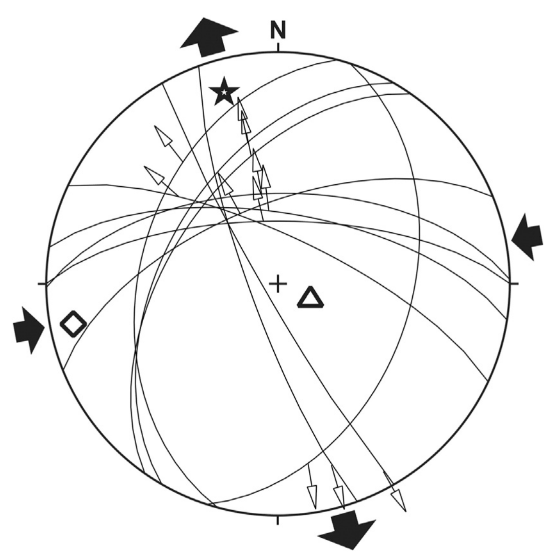

Fig. 24. Numerical inversion of the 1978 ground ruptures showing an overall good consistency with a NNW-SSE direction of extension (stress symbols as in Fig. 19; redrawn from Mercier et al. (1983)).

Please cite this article as: Caputo, R., et al., Comparison between *single-event effects* and *cumulative effects* for the purpose of seismic hazard assessment. A review from Greece, Earth-Sci. Rev. (2015), http://dx.doi.org/10.1016/j.earscirev.2015.05.004

Fig. 25. Example of co-seismic ground rupture in a tobacco field showing a typical vertical displacement of *ca.* 10 cm.

than 8 km; Hatzfeld et al., 1986/87). A mean value of 57° has thus been assumed. According to minimum and maximum depths and dip-angle, the estimated width of this ISS is ~18 km, though based Q29 on width vs length relationships (Wesnouski, 2008; Leonard, 2010) it would be only 15 and 14 km, respectively. Considering the maximum depth as seismologically well constrained, the latter values probably underestimate this fault dimension and we keep the above values.

Q30 Palaeoseismological investigations (Fig. 28; Pavlides, 1993; Cheng et al., 1994; Chatzipetros, 1998; Chatzipetros et al., 2005) confirm that the 1978 coseismic rupture reached the surface with a dip-angle of 65°–74°. Trenches also document the occurrence of at least other four linear morphogenic earthquakes, characterized by local slip-per-event values ranging between 10 and 25 cm. Taking into account the location of the trenches with respect to the fault traces geometry, these values likely underestimate the fault activity. Accordingly, a slip-per-event of 0.5 m and a mean recurrence interval of 1.0–1.5 ka are assumed as more typical values of this seismogenic structure.

Supposing to ignore the exact date of the last earthquake (e.g. 1978), palaeoseismological trenches document the occurrence of two events after 910 AD. The older is tentatively associated with the 1430 AD earthquake, therefore chronologically constraining the last event on this seismogenic source during the past 570 years and accordingly the elapsed time.

Based on the observed coseismic slips and the constrained ages of the palaeoevents, the slip-rate varies between 0.26 and 0.7 mm/a (Chatzipetros, 1998; Chatzipetros et al., 2005), thus emphasizing the lateral variability of the fault behaviour and the possible occurrence of some amount of post-seismic creep causing an over-estimation of this parameter (see discussion in Caputo et al. (2008)).

The maximum expected magnitude calculated by means of the seismic moment is 6.5 (M_w). On the other hand, using empirical relationships (Wells and Coppersmith, 1994; Pavlides and Caputo, 2004) it would be 6.6–6.7 (length vs magnitude) or 6.4–6.6 (slip vs magnitude). Considering that the greater values come from inversion of surface magnitudes (Pavlides and Caputo, 2004) the preferred maximum expected value remains 6.5 (Table 1).

3.4. Aliakmonas Fault System

Western Macedonia region is affected by an important fault system, which cuts across the orographic and morphological first-order texture of the NW-SE trending Hellenides fold-and-thrust belt (Fig. 1). Although the broader region was considered a rigid 'aseismic' block (Voidomatis, 1989; Papazachos, 1990) the May 13, 1995 Kozani–Grevena earthquake, one of the strongest events affecting northern Greece during the last decades, partly re-activated the Aliakmonas Fault System (Fig. 29).

3.4.1. Single-event effects

The causative seismogenic source of the 1995 earthquake has been clearly recognised and well located from either the macroseismic field (Fig. 30), the focal parameters (Dziewonski et al., 1996; Hatzfeld et al., 1997; Papazachos et al., 1998; Kiratzi and Louvari, 2003; Fig. 30) and the several kilometre-long coseismic ground ruptures (Fig. 31). Estimated seismic moments derived from seismological data vary from $4.9 \cdot 10^{18}$ to $7.6 \cdot 10^{18}$ N·m (Dziewonski et al., 1996; Hatzfeld et al., 1997; Ambraseys, 1999; Vannucci and Gasperini, 2003, 2004) corresponding to $M_w = 6.4$–6.5. Also numerical modelling based on DInSAR analyses (Fig. 32; Rigo et al., 2004), geodetic data (Fig. 33; Clarke et al., 1997), or seismological ones (Suhadolc et al., 2007) suggest $M_0 = 7.8 \cdot 10^{18}$ N·m (M_w ~ 6.5), $M_0 = 16.3 \cdot 10^{18}$ N·m (M_w ~ 6.7) and $M_w = 6.6$, respectively. Assuming that the 1995 earthquake was a characteristic event, a conservative value of 6.6 is considered as the maximum magnitude of this seismogenic source.

It is noteworthy that seismological data inversions for both slip (Giannakopoulou et al., 2005) and seismic moment distributions (Suhadolc et al., 2007) suggest the rupture of distinct asperities,

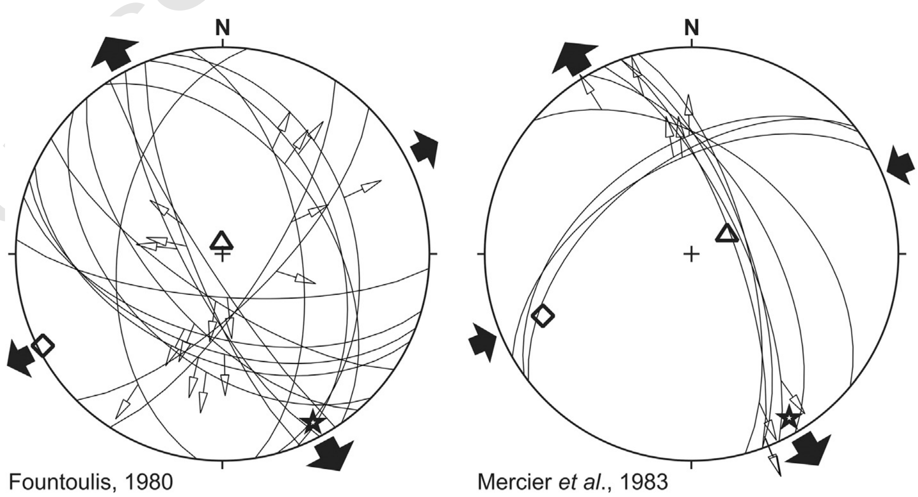

Fig. 26. Examples of numerical inversion of Quaternary fault data providing the recent principal stress directions of the broader region of the Gerakarou Fault (stress symbols as in Fig. 19). Redrawn from Fountoulis (1980) and Mercier et al. (1983).

Please cite this article as: Caputo, R., et al., Comparison between *single-event effects* and *cumulative effects* for the purpose of seismic hazard assessment. A review from Greece, Earth-Sci. Rev. (2015), http://dx.doi.org/10.1016/j.earscirev.2015.05.004

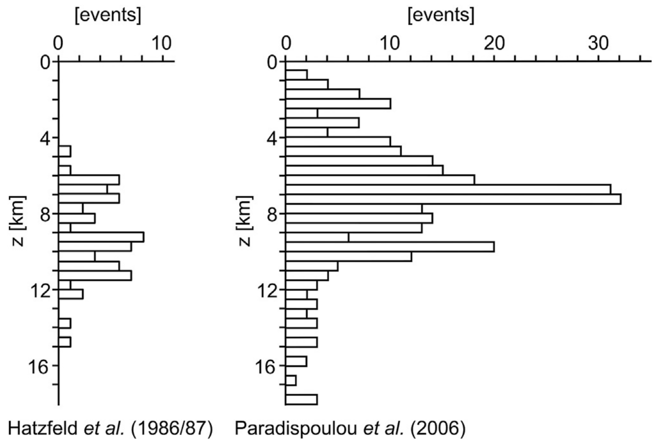

Fig. 27. Hypocentral distribution obtained from microearthquake studies within the broader seismogenic volume of the 1978 Stivos earthquake (left histogram from Hatzfeld et al. (1986/87); right from Paradisopoulou et al. (2006)) suggesting a more likely maximum depth of *ca.* 15 km (preferred value) with few exceptions.

possibly corresponding to as many fault segments (Fig. 34). Some geometrical complexities at depth are also suggested by DInSAR analyses (Meyer et al., 1996; Rigo et al., 2004; Resor et al., 2005). However, all proposed focal mechanisms (Fig. 30; Dziewonski et al., 1996; Clarke et al., 1997; Hatzfeld et al., 1997; Papazachos et al., 1998; Kiratzi and Louvari, 2003; Vannucci and Gasperini, 2003, 2004) clearly document a (E)NE-(W)SW-striking (240°–253°), NW-dipping (38°–47°), almost purely dip-slip normal fault plane (rake 259°–269°). Hypocentral aftershocks distribution (Fig. 35) and a stress tensor inversion (Kiratzi, 1999) are also in agreement with the above values. We could therefore assume that mean values (Table 1) and the possible complexities at depth are taken into account by slightly downgrading the corresponding quality factor.

As a consequence of the seismic event, several ground ruptures formed within the epicentral area (Fig. 31). The major and most continuous ones generated an ENE-WSW morphological feature, between the Rymnio and Sarakina villages, showing the northern block subsiding (Fig. 29). This independent information confirms the above parametres inferred from focal mechanisms. However, in contrast with field observations (Pavlides et al., 1995; Mountrakis et al., 1998), both satellite (Fig. 32; Meyer et al., 1996; Rigo et al., 2004; Resor et al., 2005) and geodetic techniques (Fig. 33; Clarke et al., 1997) as well as seismological data (Fig. 35; Hatzfeld et al., 1998; Papazachos et al., 1998) strongly support blind faulting for the 1995 event and suggest a minimum depth of few kilometres. Accordingly, we have tentatively assumed 1 km, but assigning a low confidence level (Table 1).

Within the uncertainty of the minimum depth and whether the faulting was blind or emergent, coseismic ground ruptures of 8–12 km (Meyer et al., 1996, 1998) or a cumulative value of *ca.* 27 km (Pavlides et al., 1995; Mountrakis et al., 1998) have been documented. The latter length is comparable with the fault length at depth inferred from DInSAR analyses (Meyer et al., 1996; Rigo et al., 2004; Resor et al., 2005), geodetic modelling (Clarke et al., 1997), aftershock spatial distribution (Hatzfeld et al., 1997) as well as forward modelling of the strong motion waveforms (Giannakopoulou et al., 2005; Suhadolc et al., 2007). A mean value of 26 km has been considered (Table 1).

As concerns the slip-per-event, the maximum displacement observed at the earth surface was less than 20 cm (Pavlides et al., 1995; Meyer et al., 1996; Mountrakis et al., 1998), but geodetic data suggest a total slip of 1.2 m (Clarke et al., 1997) and seismological inversions provide maximum and average fault slips of 2.2 and 0.7 m, respectively (Giannakopoulou et al., 2005). The latter could be considered a reasonable value (Table 1).

Spatio-temporal aftershock distribution (Hatzfeld et al., 1997) and stress tensor inversion (Kiratzi, 1999) also suggest the occurrence of an antithetic fault plane, the Chromio Fault, that was probably reactivated as a secondary inherited structure. Also this fault was associated with ground ruptures (Pavlides et al., 1995; Mountrakis et al., 1998) showing a normal kinematics (south block subsiding). Its secondary role relative to the major seismogenic source is clear and will not be further discussed.

A maximum depth of 14 km is obtained from hypocentral depths of both mainshock and aftershocks (Fig. 35; Hatzfeld et al., 1997; Chiarabba and Selvaggi, 1997; Papazachos et al., 1998). A width trigonometrically calculated from depth values and dip-angle is 19.5 km; however, geodetic (Clarke et al., 1997) and strong motion waveform modelling (Suhadolc et al., 2007) suggests a smaller width (16 and 17 km, respectively). Considering the uncertainty relative to the blind/emergent behaviour and based on the above proposed values, a width

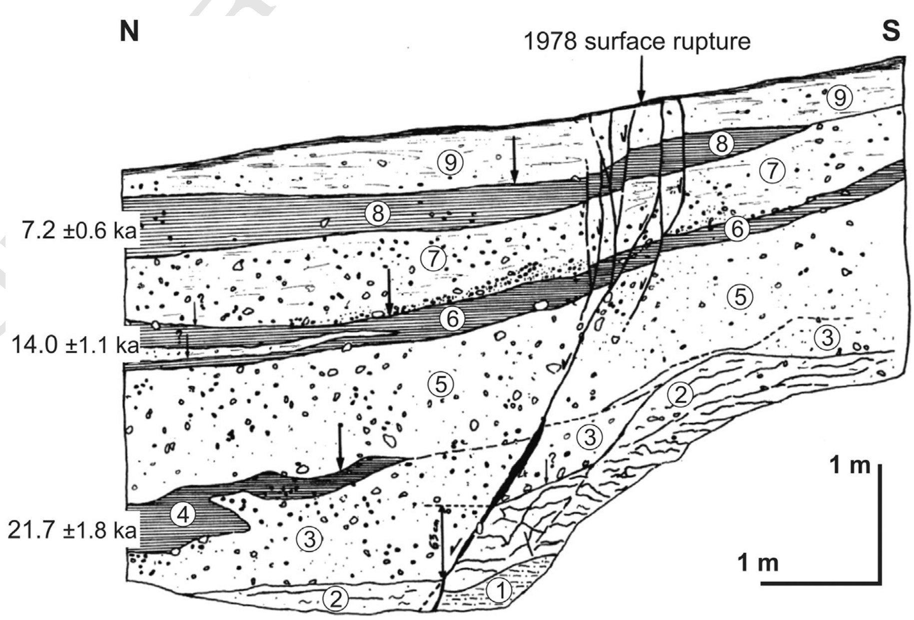

Fig. 28. Palaeoseismological trench across the Gerakarou Fault documenting the occurrence of four linear morphogenic events; numbers refer to stratigraphic units referred to in the original paper. Palaeosoils (4), (6) and (8) represent event-horizons and have been dated at *ca.* 21.7 ±, 14.0 and 7.2 ka (from Pavlides et al. (1995)). Q4

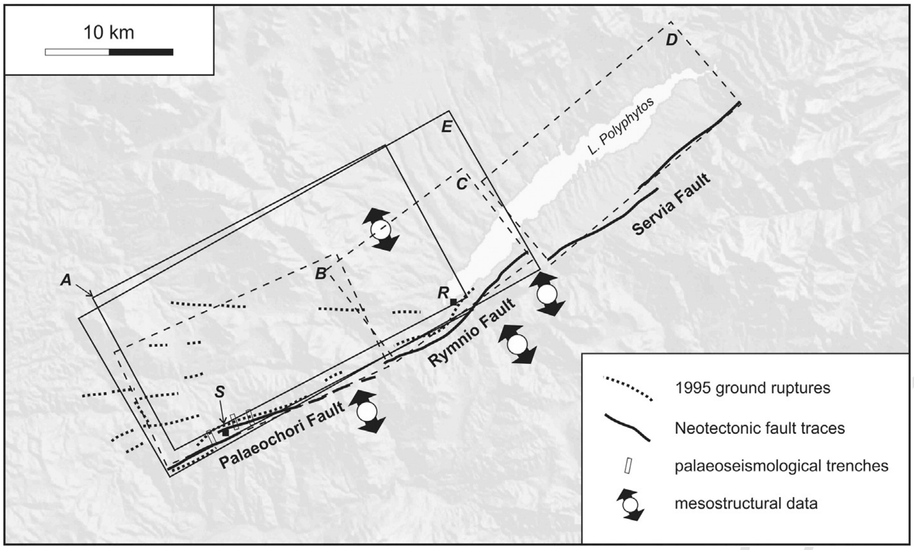

Fig. 29. Map of the Aliakmonas Fault System, Western Macedonia, showing the seismogenic source obtained from the analysis of *single-event effects* (box *A*). The analysis of the *cumulative effects* suggests the occurrence of three major segments: Palaeochori Fault (box *B*), Rymnio Fault (box *C*) and Servia Fault (box *D*). The former two are separated by a soft segment boundary and therefore they could represent a unique 'earthquake segment' (sensu dePolo et al. (1991); box *E*). The solid small black squares refer to the towns of Sarakina (*S*) and Rymnio (*R*). The Neotectonic fault traces, the 1995 ground ruptures, the location of the palaeoseimological trenches and the results of mesostructural analyses are also represented. See text for discussion and full reference list. Seismotectonic parameters of the analysed ISSs (boxes *A* and *E*) are reported in Table 1.

of 18 km has been assumed (Table 1), enabling to calculate the seismic moment which also confirms the preferred magnitude ($M_w = 6.6$) previously discussed.

3.4.2. Cumulative effects

Geological and morphotectonic investigations indicate the Aliakmonas Fault System as one of the major tectonic features affecting Western Macedonia (Fig. 29). The whole structure cuts perpendicularly across the mean orogenic trend of the Hellenides, showing clear evidences of recent activity for more than 50 km along strike. Detailed mapping emphasizes the occurrence of three major segments (Palaeochori, Rymnio and Servia faults, from SW to NE, respectively; boxes *B*, *C*, and *D* in Fig. 29). The Servia Fault shows the most prominent features of recent activity being associated with a major escarpment developed in carbonate rocks and bordering the Polyphytos Lake (Pavlides et al., 1995; Doutsos and Koukouvelas, 1998; Mountrakis et al., 1998; Goldsworthy and Jackson, 2000), while the two southwestern segments (Palaeochori and Rymnio ISSs) show discontinuous and subtle scarps, as a consequence of the affected lithologies mainly belonging to the ophiolitic suite, less conservative from a morphological point of view. The three segments have been distinguished and separated respectively in correspondence with a right-stepping underlapping geometry (Rymnio/Servia ISSs), and a slight angular boundary with a possible

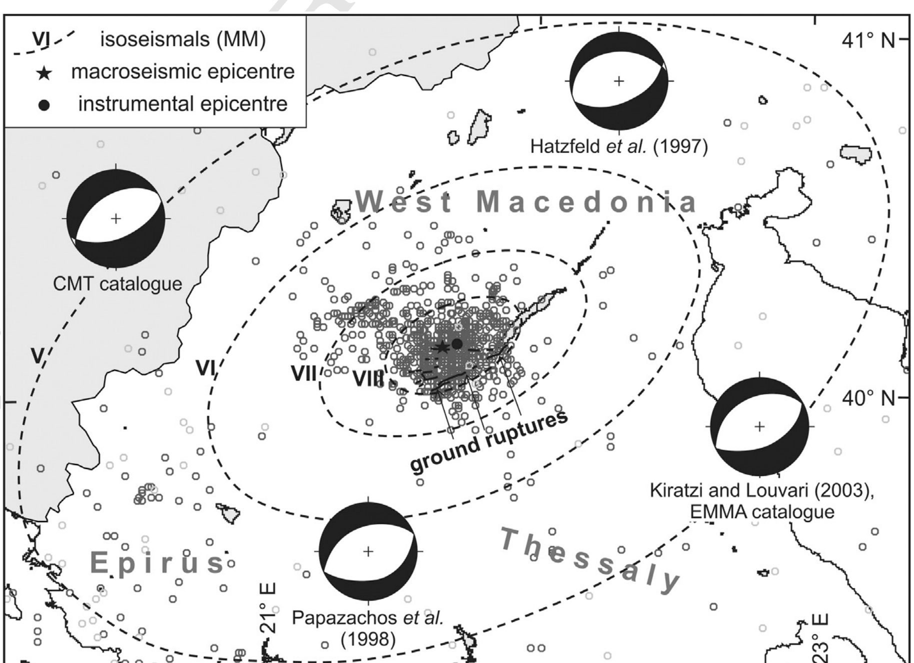

Fig. 30. Isoseismal curves, macroseismic and instrumental epicentres of the 1995 Kozani–Grevena earthquake. Some focal mechanism of the main shock as well as the foreshocks and aftershocks are also represented as light and dark grey cirlces, respectively. See text for full reference list.

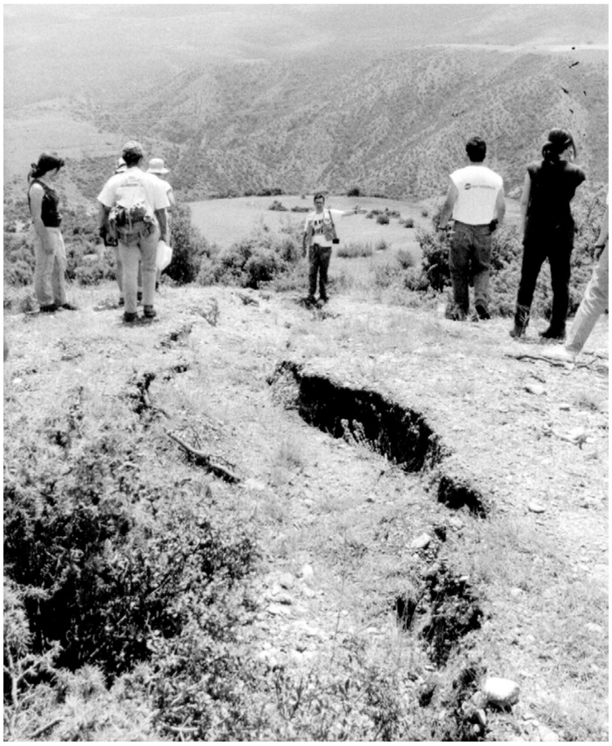

Fig. 31. Example of surface rupture near Sarakina village, affecting Neogene molasse deposits and showing a local vertical displacement of about 10 cm.

geometric gap (Palaeochori/Rymnio ISSs; Fig. 29). The latter could be defined a soft segment boundary (e.g. Walsh and Watterson, 1991; Mansfield and Cartwright, 2001) and therefore the Palaeochori and Rymnio faults could possibly behave as a unique seismogenic source. In contrast, the 2 km-large overstep between the Rymnio and Servia segments likely represents a hard boundary. For the purposes of this paper, we will thus focus on the Palaeochori and Rymnio segments. The former is characterized by ENE-WSW-striking scarps extending for a length of *ca.* 18 km and progressively disappearing towards the SW, while the latter fault extends for a total length of 14 km (Pavlides et al., 1995). A cumulative value along strike of 33 km has thus been considered with a mean strike of 242° (box *E* in Fig. 29).

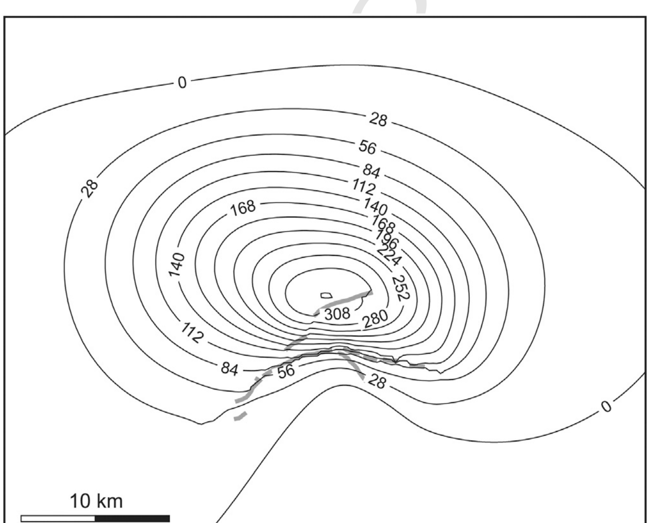

Fig. 32. The subsidence (values in mm) associated with the Kozani–Grevena earthquake as obtained from DInSAR analysis (redrawn from Rigo et al. (2004)).

Palaeoseismological investigations carried out across the Palaeochori segment (Chatzipetros, 1998; Chatzipetros, 1998) reveal the occurrence of at least three linear morphogenic events older than the 1995 earthquake (Fig. 36). Based also on the continuous ground ruptures along the morphotectonic fault trace (Fig. 29; Pavlides et al., 1995; Mountrakis et al., 1998), this seismogenic source is considered emergent and thus the minimum depth is posed at 0 km.

Seismic tomographies obtained from the aftershocks of the 1995 event (Chiarabba and Selvaggi, 1997), (however, here considered equivalent to a typical microearthquake investigation used in the *cumulative effects* approach), allow to delineate the deeper geometry of the fault characterized at depth by a moderately-dipping setting becoming progressively steeper upwards, therefore suggesting a listric geometry from which the assumed mean dip-angle is 45°. The same dataset also helps in constraining a seismogenic layer thickness of *ca.* 15 km (Hatzfeld et al., 1997; Drakatos et al., 1998).

Based on minimum and maximum depth and dip-angle, the trigonometrically obtained fault's width is 21 km. Although empirical relationships (Wesnouski 2008; Leonard, 2010) provide smaller values (between 16 and 17 km), the former procedure is more reliable and therefore a mean value of at least 20 km is assumed (Table 1)

Mesostructural analyses along the Aliakmonas Fault System (Fig. 37; Pavlides and Mountrakis, 1987; Mountrakis et al., 1998), show a (N)NW-trending direction of extension similar to the one measured in nearby structures (Ptolemaida Basin to the north; Pavlides and Mountrakis, 1987) and roughly perpendicular with the mapped fault trace, therefore constraining a mean overall dip-slip kinematics with a slight right-lateral component (i.e. rake ~265°).

The above-mentioned palaeoseismological investigations show that the amount of slip varies for different events and from trench to trench (10–80 cm) and suggest that previous coseismic ruptures were likely not always located on the same segment surface and they were probably distributed over subparallel fault strands (Fig. 36). A mean value of 0.5 m is therefore assumed with a large uncertainty.

The poorly constrained TL-datings obtained from trenches would suggest a very low slip-rate and a mean recurrence interval longer than 10 ka (and less than 30 ka; Fig. 38). However, based on geological and morphological considerations Doutsos and Koukouvelas (1998) estimate a faster long-term slip-rate (0.3 mm/a) also suggesting a much shorter recurrence interval (2 ka).

Based on the above-defined values, the slip vs magnitude and length vs magnitude empirical relationships (Wells and Coppersmith, 1994; Pavlides and Caputo, 2004) provide 6.4–6.6 and 6.9, respectively, while the moment magnitude calculated by means of the seismic moment would be between 6.6 and 6.7. Taking into account the overall uncertainties on the different parameters, a reasonable mean value of 6.7 could be considered as the maximum expected magnitude.

In this case study, the age of the last event, and hence the elapsed time, supposing to ignore the 1995 earthquake, would be very poorly constrained due to the paucity of available and reliable datings from the palaeoseismological investigations. The last rupture observed in the trenches clearly affects layers containing several pottery fragments, which are Neolithic at the oldest (i.e. 5–6 ka BP), but unfortunately have been not better defined chronologically.

4. Discussion

In order to emphasize advantages and limitations of the two approaches, we now analyse the numerical results and associated uncertainties obtained by separately exploiting the two *sources of information*, and discuss both similarities and differences for the principal seismotectonic parameters thus collected. All values are synthetically reported in Table 1 and have been lengthily discussed in the previous section.

Please cite this article as: Caputo, R., et al., Comparison between *single-event effects* and *cumulative effects* for the purpose of seismic hazard assessment. A review from Greece, Earth-Sci. Rev. (2015), http://dx.doi.org/10.1016/j.earscirev.2015.05.004

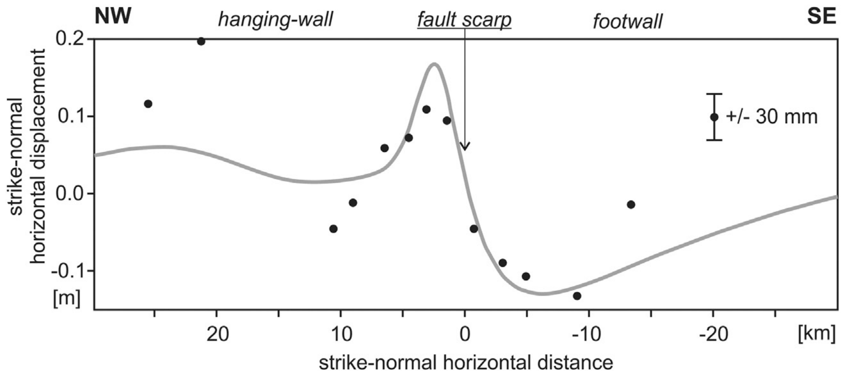

Fig. 33. Observed (dots) and modelled (solid line) horizontal site displacements along a profile normal to the Palaeochori Fault scarp (redrawn from Clarke et al. (1997)).

In the first case study, the East Heliki Fault reactivated by the 1861 Valimitika earthquake (Figs. 3 and 4), both approaches give comparable results for location, strike and minimum depth. If the kinematics can only be grossly obtained by the *single-event effects*, it is certainly more accurate based on mesostructural analyses (viz. *cumulative effects*). Similarly, the real fault length is poorly determined with the first

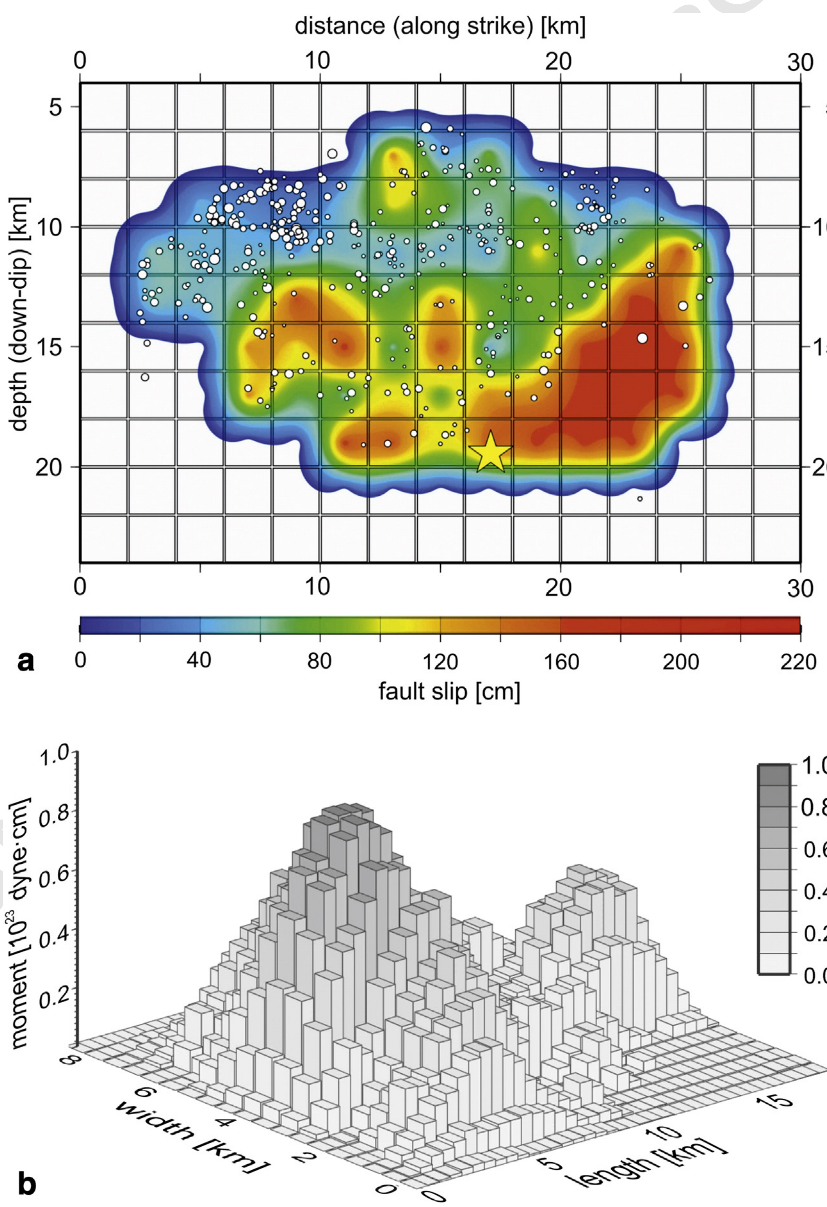

Fig. 34. Slip distribution on the fault plane relative to the 1995 Kozani–Grevena earthquake showing the ocurrence of two major slip patches (segments?) from (a) Giannakopoulou et al. (2005) and (b) Suhadolc et al. (2007).

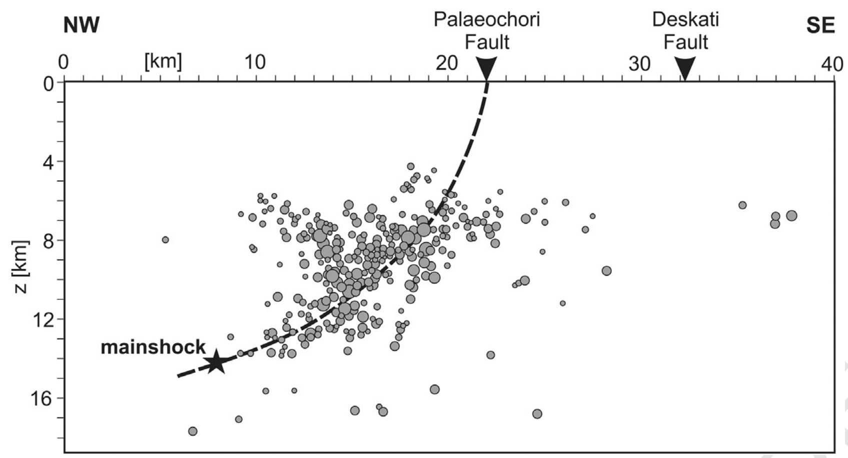

Fig. 35. Aftershocks distribution at depth along a profile normal to the Palaeochori and Deskati fault traces. Th dashed lines represents the inferred geometry of the seismogenic fault. Redrawn from Hatzfeld et al. (1998).

methodological approach, but better constrained with the second one. Palaeoseismological data match, within uncertainties, the measured surface displacement of the coseismic ground ruptures. In this case study, other parameters like width, maximum depth, dip-angle and recurrence interval could be directly derived from *cumulative effects*-based investigations, but they could be only tentatively and very roughly inferred from the *single-event effects*, using e.g. empirical relationships. Among the major differences is probably the overall size of the fault plane. As previously discussed, slip-rate and recurrence interval cannot be obtained by the first approach and this limitation stands also for the other case studies. Conversely, the timing of the last event and hence the elapsed time are not precisely determined, but they could be only chronologically constrained using 'geological' data. Finally, it is worth noting that the maximum expected magnitude is however equal within uncertainties though obtained in different ways. The maximum magnitude issue will be further discussed in the following because it represents a crucial parameter in SHA analyses.

In the second case study, the Domokos Fault System reactivated by the 1954 Sophades earthquake (Figs. 11 and 12), the analysis of the *single-event effects* provides contradicting results whether we give emphasis to the macroseismic and field information or to seismological ones (solutions represented by box *A* and *B*, respectively). Both solutions, however, have large uncertainties. Indeed, in the former case, i) macroseismic information is relatively poor for seismotectonic purposes, ii) observed ground ruptures do not fit the length and lateral continuity expected for a strong crustal earthquake on normal faults, especially in the Aegean domain (Pavlides and Caputo, 2004), and iii) two out of three of the proposed epicentres fall outside the projection of the plane. On the other hand, for the solution based on seismological information i) the proposed focal mechanism (McKenzie, 1972) is based on a poor seismological network and especially obtained from short-period recordings, ii) the location and particularly the orientation of box *B* is in manifest contrast with the first order orography of Thessaly characterized by a NW-SE trending basin-and-range-like morphology (Caputo, 1990), and iii) the suggested kinematics is not in agreement with the present-day stress-field affecting the region (Caputo and Pavlides, 1993).

If we now compare the above results with those obtained from the *cumulative effects*-based analyses (box *C* in Fig. 11), solution *B* largely differs, while solution *A* shows a better match in location, geometry and kinematics and a comparable value for the maximum expected magnitude. Slip-rate, slip per event and the recurrence interval inferred from *cumulative effects* observations (Caputo, 1995; Palyvos et al., 2010) are in good agreement with the regional strain-rate calculated from GPS measurements and other similar Aegean-type active faults in the broader area (Clarke et al., 1998; Hollenstein et al., 2008). As concerns

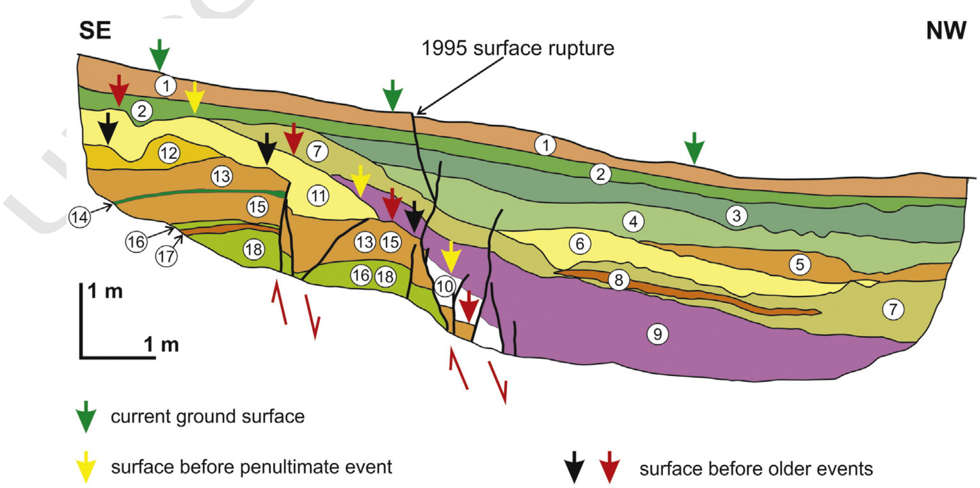

Fig. 36. Example of palaeoseismological trench across the Palaeochori fault trace associated with the 1995 earthquake (Chatzipetros et al., 1998), documenting the occurrence of older linear morphogenic events and allowing to constrain (though with different degree of uncertainty) several seismotectonic parameters (i.e. slip per event, slip-rate, recurrence, last earthquake and elapsed time).

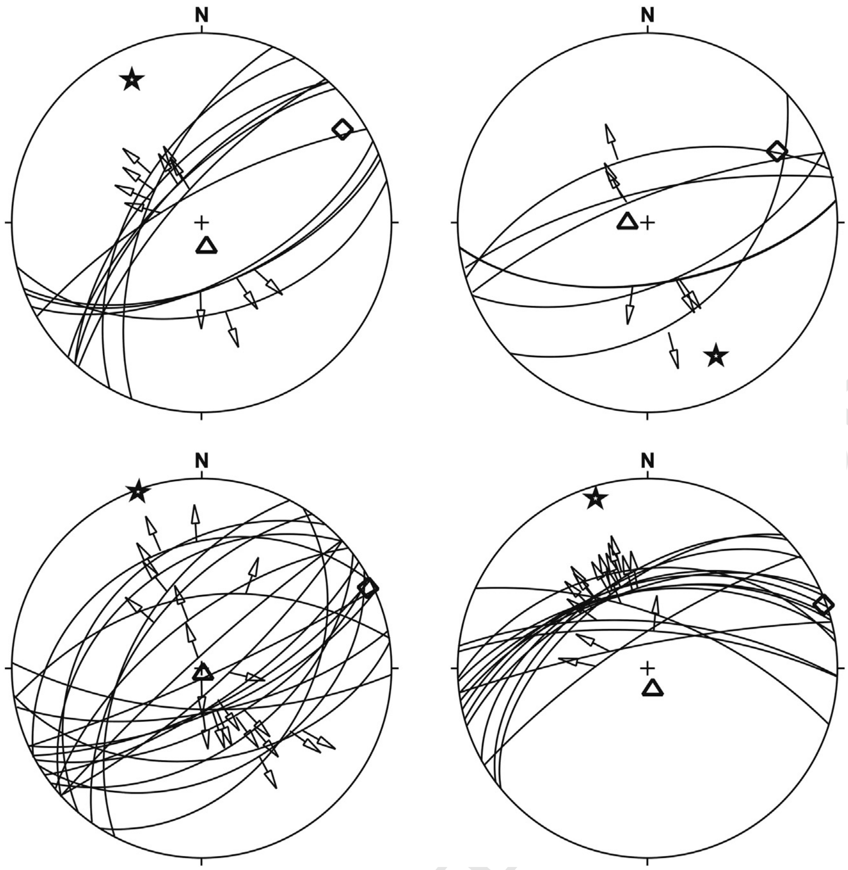

Fig. 37. Examples of mesostructural data measured in the surroundings of the Aliakmonas Fault System. The numerical inversions (stress symbols as in Fig. 19) indicate a NNW-SSE direction of extension from which a mean rake of 265° can be calculated for the fault plane represented by box *E* in Fig. 29. Redrawn from Pavlides and Mountrakis (1987) and Mountrakis et al. (1998).

the maximum expected magnitude, slightly greater for box *C*, we should consider the likely immature stage of the Domokos Fault System due to its relatively young age (Middle–Late Pleistocene to Present). As a consequence, linkage processes, unification of minor sliding surfaces originally independent and smoothing of the fault plane are still in progress, therefore the 1954 Sophades earthquake may have not ruptured the whole surface of the two central segments (Leondari and Velessiotes; Figs. 11 and 15) already behaving as a unique seismogenic source (i.e. 'fully breached relays'; Soliva and Benedicto, 2004). Future events will be possibly able to do so (i.e. worst-case scenario), therefore slightly increasing the overall amount of released energy and seismic moment.

In the third case study represented by the Gerakarou seismogenic source belonging to the Mygdonia Fault System reactivated by the 1978 Stivos earthquake (Figs. 20 and 21), the critical analysis of both *sources of information* can provide most of the investigated seismotectonic parametres. Excluding as above-mentioned some parameters (i.e. slip-rate and recurrence interval, on the one side, and timing of the last event and elapsed time, on the other side), only slight differences could be observed in the numerical values (always less than few percent) and in the degree of confidence and/or uncertainty we have attributed (see Table 1). The latter are probably intrinsic of the two followed approaches reflecting the different reliability and content of the two *sources of information* and associated investigation techniques.

Also in the fourth case study is the Aliakmonas Fault System reactivated by the 1995 Kozani–Grevena earthquake (Figs. 29 and 30), differences between the two preferred seismogenic sources (boxes *A* and *E* in Fig. 29) could be considered secondary ones with the exception of the fault length (26 km *vs* 33 km) and consequently of the maximum expected magnitude (M_w 6.6 *vs* M_w 6.7; Table 1). Here, similar to the

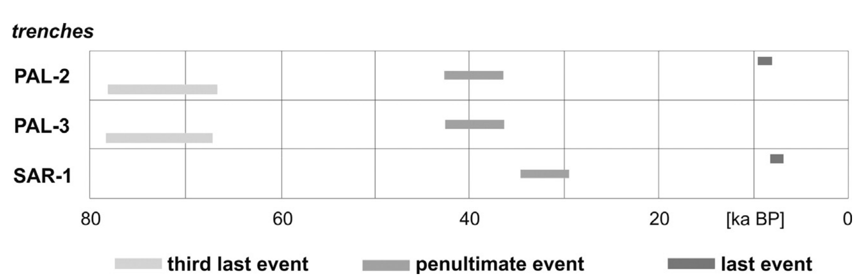

Fig. 38. Time windows for past events obtained from three different palaeoseismological trenches across the Palaeochori Fault allowing to constrain the mean recurrence interval. Redrawn from Chatzipetros et al. (1998).

Q6

Domokos Fault System and possibly several other examples in the Aegean Region (like the composite seismogenic sources Amyndeo, Ptolemaida, Anthemoundas, Stratoni–Varvara, Vasilika, Pagasitikos Gulf, Lokris, North Alkyonides Gulf, South Alkyonides Gulf, Sarandis Bay, and probably many others located in offshore settings; Caputo and Pavlides, 2013), it is likely a matter of ongoing linkage processes in young structures and a function of the evolutionary stage of these mechanically, geometrically and kinematically composite seismogenic sources. In the particular case, the 1995 Kozani–Grevena earthquake has probably ruptured most of the Palaeochori and Rymnio segments but as two major distinct asperities (Fig. 34), therefore releasing less energy (viz. smaller magnitude) than expected by a fault plane with a length corresponding to the simple sum of the two segments.

5. Concluding remarks

In this paper we presented four case studies of seismogenic sources, selected from GreDaSS (Caputo and Pavlides, 2013), which have been reactivated by historical or instrumental earthquakes. The principal aim is to discuss on some crucial methodological issues and problems typically faced in the compilation of this kind of databases. Indeed, in order to fill the lack of (good) instrumental data for events older than few decades and of historical data sufficient to provide the principal seismotectonic parameters of a specific seismogenic source, it is clear that geologically-based information must be fully exploited. For this reason, we have described and discussed how the necessary seismotectonic information can be obtained from two distinct *sources of information*, namely the *single-event effects* and the *cumulative effects*, analysing the two sets of data available for the four case studies separately and basically using different methodological approaches (Caputo and Helly, 2008). As a matter of fact the two *sources of information* focus on the same 'object', but from two distinct perspectives: the past seismic event, on the one side, and the corresponding physical source, on the other. This distinction is crucial as far as with the same methodological tools used for analysing the *cumulative effects* on seismogenic sources, it is also possible to suggest different scenarios of fault reactivation. For example, as previously discussed for the Domokos and Aliakmonas fault systems, the presence of segments, but especially their geometrical setting and the different type of segment boundaries (i.e. hard- versus soft-type) could allow the reactivation of surface ruptures of variable size that generally do not correspond to a characteristic earthquake model (Schwartz and Coppersmith, 1984). This is obviously valid for past earthquakes and it could be possibly documented on the basis of detailed and systematic palaeoseismological investigations. However, such a behaviour has also a strong impact in SHA analyses as far as the choice of the maximum magnitude significantly influences the slope and shape of the Gutenberg–Richter curve (Wesnousky, 1994;
Q35 Kagan, 1996; Molchan et al., 1997) and therefore the probability distribution of future events (e.g. Nekrasova and Kosobokov, 2006). Only dedicated and extensive investigations on the *cumulative effects* associated with seismogenic sources affecting a region may contribute to define the more appropriate frequency–magnitude distribution and hence
Q37 Q36 to decide between a gamma model (Kagan, 1991a, 1991b; Kagan, 1996), a characteristic earthquake model (Schwartz and Coppersmith, 1984; Wesnousky, 1994) or a multi-scale seismicity model (Caputo et al., 1973; Molchan et al., 1997; Nekrasova et al., 2011).

For the exercise of this note, which is mainly devoted to compare the two approaches, we assumed a characteristic earthquake model and the tectonic structures here analysed, described and characterized in terms of seismotectonic parameters (see Table 1) correspond to *individual seismogenic sources* (Basili et al., 2008). As mentioned in Section 1, since several years the *composite seismogenic sources*, CSSs, have been introduced also in GreDaSS (Caputo and Pavlides, 2013). In this regard, three out of four CSSs which include the ISSs discussed in this paper are indeed associated with a greater value of the maximum expected magnitude (http://gredass.unife.it).

The case studies have been selected diachronically starting from the 1861 Valimitika earthquake, which represents the first example for Greece of penecontemporaneous systematic field investigations complete of a detailed ground rupture map and scientific report of many seismically induced effects (Schmidt, 1867, 1879). The subsequent three case studies are not only progressively more recent, but also all Q38
represent instrumentally recorded events that occurred in different stages of the technological evolution (1954 Sophades, 1978 Stivos and 1995 Kozani–Grevena earthquakes). Thereupon, it was also possible to emphasize the differences, in both quality and quantity, of the results obtained from *single-event effects*-based investigations. For example, the Sophades event occurred at the dawn of the Greek seismographic network development when the international one was still in an embryonic phase. Conversely, during the 1995 Kozani–Grevena event Q39
the national and regional networks were highly improved in terms of used technology and architecture, while other *single-event effects* investigation techniques, like GPS surveys and InSAR analyses, started to be available to researchers.

In practice the key limitations of the two approaches are the following. On the one side, *single-event effects* cannot intrinsically provide either the slip-rate or the recurrence interval, unless the specific seismogenic source is characterized by very short recurrence intervals, historically well documented, which is commonly not the case for the Aegean Region and most active faults of the broader Mediterranean realm. On the other hand, the methodological approaches generally applied to analyse *cumulative effects* are usually not able to sufficiently constrain the timing of the last linear morphogenic earthquake (Caputo, Q40
2005) and consequently of the elapsed time.

According to the above discussion and comparing the results shown in Table 1, two major conclusions follow. Firstly, the decreasing reliability and increasing degree of uncertainty with increasing age of the historical and instrumental event, relative to the seismotectonic parameters obtained from the analysis of *single-event effects* are evident. De facto, instrumental information is not available for events older than one century the maximum and even macroseismic information rapidly fades with the past time. Secondly, if it is reasonable that information inferred from the analysis of *cumulative effects* Q41
for the most recent events, especially when recorded by multiple high-technology apparati, has a slightly lower rank (see Table 1), it is conversely noteworthy that this 'geological' approach always gives a satisfactory quality level, even for older events either pre-instrumental and pre-historic. In this regard, the degree of uncertainty or reliability generally depend on the quality (and quantity) of dedicated investigations carried out on the specific fault. The latter issue is obviously a matter of research funding, but sometimes it is also a matter of bias which affects the researchers. Indeed, in the Aegean Region several faults capable of generating earthquakes with $M_w > 5.5$ are probably to be recognised yet, but for researchers it is certainly more appealing and apparently more gratifying to investigate 'famous' seismogenic sources than poorly known ones.

Another important difference between the two *sources of information* is due to the fact that the analysis of the various *cumulative effects* could be generally repeated as many times as desired and, in principle, they can be carried out by any researcher for their possible scientific falsification. Also, the progressively improving technology and the increasing geological and seismotectonic knowledge may further potentially reduce the degree of uncertainty of the information obtained with this approach. In contrast, *single-event effects* are fundamentally unique, that is to say if a seismometer or a satellite has some temporary default (alternatively, the seismographic network or the InSAR imageries are not sufficiently dense at the time of the earthquake) there is no second chance to obtain again the particular information belonging to the *single-event effects*.

In conclusion, even if the analysis of *cumulative effects* could provide a 'resolution' somehow lower than the other approach (but only if compared with most very recent earthquakes), its applicability is incomparably much larger and the associated techniques could be potentially and systematically applied to a huge number of seismogenic sources and capable faults. For these reasons, the analysis of *cumulative effects* certainly represents a much more powerful tool for seismotectonic investigations and for the compilation of a database to be fully exploited for SHA analyses, like DISS (DISS WG, 2010; Basili et al., 2013), GreDaSS (Caputo and Pavlides, 2013) and EDSF (Basili et al., 2013).

This advantage becomes dominant when performing seismotectonic investigations in geodynamic regions like the Aegean characterized by numerous active or potentially active faults (capable faults) that have been not reactivated by a recent earthquake (i.e. included in historical and/or instrumental catalogues). This is mainly due to the generally long recurrence interval, say several centuries up to some thousands years, characterizing the Aegean Region. As a consequence, these tectonic structures are likely associated with a higher level of seismic hazard and hence are certainly much more dangerous than the recently reactivated seismogenic sources. From this point of view, this research could be also considered as an attempt to calibrate the reliability of the different methodological approaches applied to the analysis of *cumulative effects* and particularly for understanding the degree of uncertainty of the obtained seismotectonic parameters. We feel that this exercise was successful in definitely showing the importance and crucial role played by the 'geological' information and its full exploitation for the purpose of compiling a database of seismogenic sources. Indeed, focusing on geological investigations will progressively improve database completeness, both in terms of recognised seismogenic sources and their principal seismotectonic parameters, and therefore probabilistic SHA analyses will certainly improve and deterministic ones will likely proliferate more and more.

Q42
6. Uncited references

Ambraseys, 2009
Angelier, 1979
Brooks and Williams, 1982
Ch and King, 1983
Chatzipetros et al., 2004
Guidoboni and Comastri, 2005
Hancock and Barka, 1987
Hatzfeld, 1999
Kanamori and Anderson, 1975
Kokkalas et al., 2006
Le Pichon and Angelier, 1981
Le Pichon et al., 1995
Lybéris, 1984
McKenzie, 1978
McNeill and Ll, 2004
Mercier, 1977
Mercier and Gailhardis, 1989
Mercier et al., 1989
North, 1977
Panagiotopoulos et al., 1993
Papanastassiou, 2001
Papazachos and Comninakis, 1982
Papazachos and Kiratzi, 1996
Papazachos et al., 2001
Stewart and Hancock, 1991
Taymaz et al., 1991
Voidomatis et al., 1990

Acknowledgements

Roberto Basili and Gianluca Valensise (INGV, Rome) are warmly thanked for providing the DISS software, its continuous maintenance and for the numerous discussions on seismogenic fault issues. The financial assistance provided by the Italian Ministry of University and Research to SS and RC is acknowledged.

References

Ambraseys, N.N., 1999. Early earthquakes in the Kozani area, northern Greece. Tectonophysics 308, 291–298. http://dx.doi.org/10.1016/S0040-1951(99)00077-3.
Ambraseys, N.N., 2001. Reassessment of earthquakes, 1900–1999, in the Eastern Mediterranean and the Middle East. Geophys. J. Int. 145, 471–485.
Ambraseys, N., 2009. Earthquakes in the Mediterranean and Middle East: A Multidisciplinary Study of Seismicity up to 1900. Cambridge University Press (968 pp.).
Ambraseys, N.N., Jackson, J.A., 1990. Seismicity and associated strain of central Greece between 1890 and 1988. Geophys. J. Int. 101, 663–708.
Ambraseys, N.N., Jackson, J.A., 1997. Seismicity and strain in the Gulf of Corinth (Greece) since 1694. J. Earthq. Eng. 1 (3), 433–474.
Ambraseys, N.N., Jackson, J.A., 1998. Faulting associated with historical and recent earthquakes in the Eastern Mediterranean region. Geophys. J. Int. 133, 390–406.
Angelier, J., 1979. Recent Quaternary tectonics in the Hellenic arc: examples of geological observations on land. Tectonophysics 52, 267–275.
Barker, J.S., Langston, C.A., 1981. Inversion of teleseismic body waves for the moment tensor of the 1978 Thessaloniki, Greece, earthquake. Bull. Seismol. Soc. Am. 71, 1423–1444.
Basili, R., Valensise, G., Vannoli, P., Burrato, P., Fracassi, U., Mariano, S., Tiberti, M.M., Boschi, E., 2008. The database of individual seismogenic sources (DISS), version 3: summarizing 20 years of research on Italy's earthquake geology. Tectonophysics 453 (1–4), 20–43.
Basili, R., Kastelic, V., Demircioglu, M.B., Garcia, Moreno D., Nemser, E.S., Petricca, P., Sboras, S.P., Besana-Ostman, G.M., Cabral, J., Camelbeeck, T., Caputo, R., Danciu, L., Domac, H., Fonseca, J., García-Mayordomo, J., Giardini, D., Glavatovic, B., Gulen, L., Ince, Y., Pavlides, S., Sesetyan, K., Tarabusi, G., Tiberti, M.M., Utkucu, M., Valensise, G., Vanneste, K., Vilanova, S., Wössner, J., 2013. The European Database of Seismogenic Faults (EDSF) compiled in the framework of the Project SHARE. http://diss.rm.ingv.it/share-edsf/.
Bell, R.E., McNeill, L.C., Bull, J.M., Henstock, T.J., 2008. Evolution of the offshore western Gulf of Corinth. Bull. Geol. Soc. Am. 120, 156–178.
Bernard, P., Briole, P., Meyer, B., Lyon-Caen, H., Gomez, J.-M., Tiberi, C., Berge, C., Cattin, R., Hatzfeld, D., Lachet, C., Lebrun, B., Deschamps, A., Courboulex, F., Larroque, C., Rigo, A., Massonnet, D., Papadimitriou, P., Kassaras, J., Diagourtas, D., Makropoulos, K., Veis, G., Papazisi, E., Mitsakaki, C., Karakostas, V., Papadimitriou, E., Papanastassiou, D., Chouliaras, G., Stavrakakis, G., 1997. The Ms = 6.2, June 15, 1995, Aigion earthquake (Greece): evidence for low angle normal faulting in the Corinth rift. J. Seismol. 1, 131–150. http://dx.doi.org/10.1023/A:1009795618839.
Catalogo dei forti terremoti in Italia dal 461 a.C. al 1990, 2. In: Boschi, E., Guidoboni, E., Ferrari, G., Valensise, G., Gasperini, P. (Eds.), ING-SGA, Bologna (644 pp.).
Bourouis, S., Cornet, F.H., 2009. Microseismic activity and fluid fault interactions: some results from the Corinth Rift Laboratory (CRL) Greece. Geophys. J. Int. 178 (1), 561–580. http://dx.doi.org/10.1111/j.1365-246X.2009.04148.x.
Brooks, M., Williams, G.D., 1982. Extensional tectonics in Neogene and Quaternary sequences at the western margin of the Axios basin, northern Greece. J. Geol. Soc. London 139, 293–297.
Bull, W.B., 2009. Tectonically Active Landscapes. Wiley-Blackwell (326 pp.).
Burbank, D.W., Anderson, R.S., 2001. Tectonic Geomorphology. Blackwell Science (274 pp.).
Camassi, R., Stucchi, M., 1997. *NT4.1: un catalogo parametrico di terremoti di area italiana al di sopra della soglia del danno (versione NT4.1.1 luglio 1997)*. Milano, rapporto tecnico GNDT. http://emidius.mi.ingv.it/NT/home.html (86 pp., last visited July 2006).
Caputo, R., 1990. Geological and structural study of the recent and active brittle deformation of the Neogene–Quaternary basins of Thessaly (Greece). Scientific Annals 12. Aristotle University of Thessaloniki, Thessaloniki (2 vol., 5 encl., 252 pp.).
Caputo, R., 1995. Inference of a seismic gap from geological data: Thessaly (Central Greece) as a case study. Ann. Geofis. 38, 1–19.
Caputo, R., Helly, B., 2005. Archaeological evidences of past earthquakes: a contribution to the SHA of Thessaly, Central Greece. J. Earthq. Eng. 9 (2), 199–222.
Caputo, R., Helly, B., 2008. The use of distinct disciplines to investigate past earthquakes. Tectonophysics 453 (1–4), 7–19. http://dx.doi.org/10.1016/j.tecto.2007.05.007.
Caputo, R., Pavlides, S., 1993. Late Cainozoic geodynamic evolution of Thessaly and surroundings (central-northern Greece). Tectonophysics 223, 339–362.
Caputo, R., Pavlides, S., 2013. The Greek Database of Seismogenic Sources (GreDaSS), version 2.0.0: a compilation of potential seismogenic sources (Mw > 5.5) in the Aegean Region. http://gredass.unife.it http://dx.doi.org/10.15160/unife/gredass/0200.
Caputo, M., Keilis-Borok, V.I., Kronrod, T.L., Molchan, G.M., Panza, G.F., Piva, A., Podgactskaja, V.M., Postpischl, D., 1973. Models of earthquake occurrence and isoseismals in Italy. Ann. Geofis. 26 (2–3), 421–444.
Caputo, R., Mucciarelli, M., Pavlides, S., 2008. Magnitude distribution of linear morphogenic earthquakes in the Mediterranean region: insights from palaeoseismological and historical data. Geophys. J. Int. 174, 930–940.
Caputo, R., Hinzen, K.-G., Liberatore, D., Schreiber, S., Helly, B., Tziafalias, A., 2010. Quantitative archaeoseismological investigation of the Great Theatre of Larissa, Greece. Bull. Earthq. Eng. 9, 347–366. http://dx.doi.org/10.1007/s10518.010.9206.6.
Caputo, R., Chatzipetros, A., Pavlides, S., Sboras, S., 2012. The Greek Database of Seismogenic Sources (GreDaSS): state-of-the-art for Northern Greece. Ann. Geophys. 55 (5), 859–894. http://dx.doi.org/10.4401/ag-5168.
Carver, D., Bollinger, G.A., 1981. Aftershocks of the June 20, 1978 Greece earthquake: a multimode faulting sequence. Tectonophysics 73, 343–363.

Ch, Soufleris, King, G., 1983. A source study of the largest foreshock (on May 23) and the mainshock (on June 20) of the Thessaloniki 1978 earthquake sequence. In: Papazachos, B.C., Carydis, P.G. (Eds.), *The Thessaloniki, Northern Greece, earthquake of June 20, 1978 and its seismic sequence*, Technical Chamber of Greece, pp. 201–222.

Chatzipetros, A., 1998. Paleoseismological and morphotectonic study of the active fault systems at Mygdonia basin, eastern Chalkidiki and Kozani–Grevena [in Greek]. (PhD Thesis), Aristotle University of Thessaloniki, Greece (354 pp.).

Chatzipetros, A., Pavlides, S., Mourouzidou, O., 2004. Re-evaluation of Holocene earthquake activity in Mygdonia basin, Greece, based on new paleoseismological results. 5th Int. Symp. East. Mediterr. Geol., Ref: S2-15.

Chatzipetros, A., Kokkalas, S., Pavlides, S., Koukouvelas, I., 2005. Palaeoseismic data and their implications for active deformation in Greece. J. Geodyn. 40 (2–3), 170–188. http://dx.doi.org/10.1016/j.jog.2005.07.005.

Cheng, S., Fang, Z., Pavlides, S., Chatzipetros, A., 1994. Preliminary study of paleoseismicity of the southern Langada–Volvi basin margin fault zone, Thessaloniki, Greece. Bull. Geol. Soc. Greece 30 (1), 401–407.

Chery, J., 2001. Core complex mechanics: from the Gulf of Corinth to the Snake Range. Geology 29, 439–442.

Chiarabba, C., Selvaggi, G., 1997. Structural central on fault geometry: example of the Grevena Ms 6.6, normal faulting earthquake. J. Geophys. Res. 102, 22 445–22 457.

Cianetti, S., Tinti, E., Giunchi, C., Cocco, M., 2008. Modelling deformation rates in the western Gulf of Corinth: rheological constraints. Geophys. J. Int. 174, 749–757.

Clarke, P., Paradisis, D., Briole, P., England, P., Parson, B., Billiris, H., Veis, G., Ruegg, J.-C., 1997. Geodetic investigation of the 13 May 1995 Kozani–Grevena (Greece) earthquake. Geophys. J. Int. 135, 195–214.

Clarke, P.J., Davies, R.R., England, P.C., Parsons, B., Billiris, H., Paradissis, D., Veis, G., Cross, P.A., Denys, P.H., Ashkenazi, V., Bingley, R., Kahle, H.-G., Müller, M.V., Briole, P., 1998. Crustal strain in central Greece from repeated GPS measurements in the interval 1989–1997. Geophys. J. Int. 135 (1), 195–214.

De Martini, P.M., Pantosti, D., Palyvos, N., Lemeille, F., McNeill, L., Collier, R., 2004. Slip rates of the Aigion and Eliki faults from uplifted marine terraces, Corinth Gulf Greece. C. R. Geosci. 336, 325–334. http://dx.doi.org/10.1016/j.crte.2003.12.006.

dePolo, G., Clark, D., Slemmons, D., Ramelli, A., 1991. Historical surface faulting in the Basin and Range province, Western North America: implication for fault segmentation. J. Struct. Geol. 13, 123–136.

DISS Working Group, 2010. Database of Individual Seismogenic Sources (DISS), Version 3.1.1: a compilation of potential sources for earthquakes larger than M 5.5 in Italy and surrounding areas. http://diss.rm.ingv.it/diss/ http://dx.doi.org/10.6092/ingv.it-DISS3.1.1 (© INGV 2010 - Istituto Nazionale di Geofisica e Vulcanologia).

Doutsos, T., Koukouvelas, I., 1998. Fractal analysis of normal faults in northwestern Aegean area, Greece. J. Geodyn. 26 (2–4), 197–216.

Doutsos, T., Poulimenos, G., 1992. Geometry and kinematics of active faults and their seismotectonic significance in the western Corinth–Patras rift (Greece). J. Struct. Geol. 14, 689–699. http://dx.doi.org/10.1016/0191-8141(92)90126-H.

Drakatos, G., Papanastassiou, D., Papadopoulos, G., Skafida, H., Stavrakakis, G., 1998. Relationship between the 13 May 1995 Kozani–Grevena (NWGreece) earthquake and the Polyphyto artificial lake. Eng. Geol. 51, 65–74.

Dziewonski, A.M., Ekström, G., Franzen, J.E., Woodhouse, J.H., 1987. Global seismicity of 1978: centroid–moment tensor solutions for 512 earthquakes. Phys. Earth Planet. Inter. 46, 316–342.

Dziewonski, A.M., Ekström, G., Salganik, M.P., 1996. Centroid–moment tensor solutions for April–June 1995. Phys. Earth Planet. Inter. 96, 1–13.

Exadaktylos, G.E., Vardoulakis, I., Stavropoulou, M.C., Tsombos, P., 2003. Analogue and numerical modeling of normal fault patterns produced due to slip along a detachment zone. Tectonophysics 376, 117–134.

FAUST, 2001. *FAUlts as a Seismological Tool, European Union Environment project*. Final Report. http://www.ingv.it/~roma/banche/catalogo_europeo/index.html (ENV4-CT97-0528).

Flotte´, N., Sorel, D., Muller, C., Tensi, J., 2005. Along strike changes in the structural evolution over a brittle detachment fault: Example of the Pleistocene Corinth–Patras rift (Greece). Tectonophysics 403, 77–94.

Flotte, N., Sorel, D., 2001. Structural cross sections through the Corinth–Patras detachment fault system in Northern Peloponnesus (Aegean Arc, Greece). Bull. Geol. Soc. Greece 34 (1), 235–241.

Fountoulis, D., 1980. Etude nétectonique et sésmotectonique du bassin de Langadha (Macédoine, Grèce), thèse 3e cycle. Univ. de Paris-Sud, Paris.

Galanis, O.C., Papazachos, C.B., Hatzidimitriou, P.M., Scordilis, E.M., 2004. Application of 3-D velocity models and ray tracing in double difference earthquake location algorithms: application to the Mygdonia basin (northern Greece). Bull. Geol. Soc. Greece 36 (3), 1396–1405.

Galanopoulos, A.G., 1959. Macroseismic evidence for the fault plane. Ann. Geofis. 12 (2), 189–196.

Galanopoulos, A.G., 1960. A Catalogue of Shocks with Io ≥ VII or M ≥ 5 for the Years 1801–1958. Seismol. Lab. Univ. Athens Publ (119 pp.).

Q43 Galanopoulos, A.G., 1961. A catalogue of shocks with I° = VI for the years prior to 1800. pp. 1–19 (Athens).

Gautier, S., Latorre, D., Virieux, J., Deschamps, A., Skarpelos, C., Sotiriou, A., Serpetsidakis, A., Tselentis, A., 2006. A new passive tomography of the Aigion Area (Gulf of Corinth, Greece) from the 2002 data set. Pure Appl. Geophys. 163, 431–453.

Giannakopoulou, E.S., Papadimitriou, E.E., Karakostas, V.G., Kiratzi, A.A., 2005. Slip distribution on the fault surface of the strong earthquake (Mw 6.6) Kozani–Grevena and correlation of the aftershock activity with the static stress change (Coulomb). Workshop “The Kozani earthquake 10 years after”, Kozani, May 13–16, 2005, pp. 2–3 (Abstracts,[in Greek]).

Goldsworthy, M., Jackson, J., 2000. Active normal fault evolution in Greece revealed by geomorphology and drainage patterns. J. Geol. Soc. London 157, 967–981.

Guidoboni, E. (Ed.), 1989. I terremoti prima del Mille in Italia e nell'area mediterranea. I.N.G., Bologna (765 pp.).

Guidoboni, E., Comastri, A., 2005. Catalogue of Earthquakes and Tsunamis in the Mediterranean Area from the 11th to the 15th Century. INGV'SGA, Bologna (1037 pp.).

Guidoboni, E., Comastri, A., Traina, G., 1994. Catalogue of Ancient Earthquakes in the Mediterranean Area up to 10th Century. INGV-SGA, Bologna (504 pp.).

Hancock, P.L., Barka, A.A., 1987. Kinematic indicators on active normal faults in western Turkey. J. Struct. Geol. 9 (5–6), 573–584.

Hanks, T.C., Beroza, G.C., Toda, S., 2012. Have recent earthquakes exposed flaws in or misunderstandings of probabilistic seismic hazard analysis? Seismol. Res. Lett. 83 (5), 759–764. http://dx.doi.org/10.1785/0220120043.

Hatzfeld, D., 1999. The present-day tectonics of the Aegean as deduced from seismicity. In: Durand, B., Jolivet, L., Horvath, E., Séranne, M. (Eds.), *The Mediterranean Basins: Tertiary Extension within the Alpine Orogen*. Geol. Soc. London, Sp. Publ. 156, pp. 415–426

Hatzfeld, D., Christodoulou, A.A., Scordilis, E.M., Panagiotopoulos, D., Hatzidimitriou, P.M., 1986/87. A microearthquake study of the Mygdonian graben (northern Greece). Earth Planet. Sci. Lett. 81, 379–396.

Hatzfeld, D., Karakostas, V., Ziazia, M., Selvaggi, G., Lebogne, S., Berge, C., Guiguet, R., Paul, A., Voidomatis, P., Diagourtas, D., Kassaras, I., Koutsikos, I., Makropoulos, K., Azzara, R., Di Bona, M., Baccheschi, S., Bernard, P., Papaioannou, C., 1997. The Kozani–Grevena (Greece) earthquake of 13 May 1995 revisited from a detailed seismological study. Bull. Seismol. Soc. Am. 87 (2), 463–473.

Hatzfeld, D., Karakostas, V., Ziazia, M., Selvaggi, G., Lebogne, S., Berge, C., Makropoulos, K., 1998. The Kozani–Grevena (Greece) earthquake of May 13, 1995, a seismological study. J. Geodyn. 26 (2–4), 245–254.

Hatzfeld, D., Ziazia, M., Kementzetzidou, D., Hatzidimitriou, P., Panagiotopoulos, D., Makropoulos, K., Papadimitriou, P., Deschamps, A., 1999. Microseismicity and focal mechanisms at the western termination of the North Anatolian Fault and their implications for continental tectonics. Geophys. J. Int. 137, 891–908.

Hollenstein, C., Müller, M.D., Geiger, A., Kahle, H.-G., 2008. Crustal motion and deformation in Greece from a decade of GPS measurements, 1993–2003. Tectonophysics 449, 17–40.

Kagan, Y.Y., 1991a. Seismic moment distribution. Geophys. J. Int. 106, 123–134.

Kagan, Y.Y., 1991b. Statistics of characteristic earthquakes. Bull. Seismol. Soc. Am. 83 (1), 7–24.

Kagan, Y.Y., 1996. Comment on “The Gutenberg–Richter or characteristic earthquake distribution, which is it?” by S.G. Wesnousky. Bull. Seismol. Soc. Am. 86 (1A), 274–285.

Kagan, Y.Y., Jackson, D.D., 2013. Tohoku earthquake: a surprise? Bull. Seismol. Soc. Am. 103 (2B), 1181–1194. http://dx.doi.org/10.1785/0120120110.

Kanamori, D.H., Anderson, D.L., 1975. Theoretical basis of some empirical relations in seismology. Bull. Seismol. Soc. Am. 65, 1073–1095.

Karakaisis, G.F., Papazachos, C.B., Scordilis, E.M., 2010. Seismic sources and main seismic faults in the Aegean and surrounding area. Bull. Geol. Soc. Greece 43 (4), 2026–2042.

Kato, N., Hirasawa, T., 1996. Effects of strain rate and strength nonuniformity on the slip nucleation process: a numerical experiment. Tectonophysics 265, 299–311.

Kementzetzidou, D., 1996. Étude sismotectonique du systéme Thessalie-iles Sporades (Gréce centrale). (PhD Thesis), Observatoire de Grenoble (151 pp.).

Kiratzi, A.A., 1999. Stress tensor inversion in Western Greece using earthquake focal mechanisms from the Kozani–Grevena 1995 seismic sequence. Ann. Geofis. 42 (4), 725–734.

Kiratzi, A., Louvari, E., 2003. Focal mechanisms of shallow earthquakes in the Aegean Sea and the surrounding lands determined by waveform modelling: a new database. J. Geodyn. 36, 251–274.

Kockel F. and Mollat H. (1977): *Erläterungen zur Geologischen Karte der Chalkidiki und angrenzender Gebiete 1:100.000 (Nord Griechenland)*. Bundesanstalt für Geowissenschaften und Ruhstoffe, Hannover.

Kokkalas, S., Koukouvelas, I.K., 2005. Fault-scarp degradation modeling in central Greece: the Kaparelli and Eliki faults (Gulf of Corinth) as a case study. J. Geodyn. 40, 200–215. http://dx.doi.org/10.1016/j.jog.2005.07.006.

Kokkalas, S., Xypolias, P., Koukouvelas, I., Doutsos, T., 2006. Postcollisional contractional and extensional deformation in the Aegean region. In: Dilek, Y., Pavlides, S. (Eds.), Postcollisional tectonics and magmatism in the Mediterranean region and Asia. *Geol. Soc. Am.*, Special Paper 409, pp. 97–123.

Kontoes, C., Elias, P., Sykioti, O., Briole, P., Remy, D., Sachpazi, M., Veis, G., Kotsis, I., 2000. Displacement field and fault modeling for the September 7, 1999 Athens earthquake inferred from Ers-2 satellite radar interferometry. Geophys. Res. Lett. 27, 3989–3992.

Koukouvelas, I., Stamatopoulos, L., Katsonopoulou, D., Pavlides, S., 2001. A palaeoseismological and geoarchaeological investigation of the Eliki fault, Gulf of Corinth, Greece. J. Struct. Geol. 23, 531–543. http://dx.doi.org/10.1016/S0191-8141(00)00124-3.

Koukouvelas, I.K., Katsonopoulou, D., Soter, S., Xypolias, P., 2005. Slip rates on the Helike Fault, Gulf of Corinth, Greece: new evidence from geoarchaeology. Terra Nova 17, 158–164.

Kulhánek, O., Meyer, K., 1979. Source parameters of the Volvi–Langadhas Earthquake of June 20, 1978 deduced from body-wave spectra at stations Uppsala and Kiruna. Bull. Geol. Soc. Am. 69 (4), 1289–1294.

Le Meur, H., Virieux, J., Podvin, P., 1997. Ann. Geophys. 40 (1), 1–24.

Le Pichon, X., Angelier, J., 1981. The Aegean Sea. Philos. Trans. R. Soc. Lond. 300, 357–372.

Le Pichon, X., Chamot-Rooke, N., Lallemant, S., Noomen, R., Veis, G., 1995. Geodetic determination of the kinematics of central Greece with respect to Europe: implications for eastern Mediterranean tectonics. J. Geophys. Res. 100 (B7), 12675–12690.

Lekkas, E., 2001. The Athens earthquake (7 September 1999): intensity distribution and controlling factors. Eng. Geol. 59, 297–311.

Leonard, M., 2010. Earthquake fault scaling: self-consistent relating of rupture length, width, average displacement, and moment release. Bull. Seismol. Soc. Am. 100 (5A), 1971–1988. http://dx.doi.org/10.1785/0120090189.

Li, C., Pang, J., Zhang, Z., 2012. Characteristics, geometry, and segmentation of the surface rupture associated with the 14 April 2010 Yushu Earthquake, Eastern Tibet, China. Bull. Seismol. Soc. Am. 102 (4), 1618–1638. http://dx.doi.org/10.1785/0120110261.

Lunina, O.V., Caputo, R., Gladkova, A.A., Gladkov, A.S., 2014. Southern East Siberia Pliocene–Quaternary faults: database, analysis and inference. Geosci. Front. 5, 605–619. http://dx.doi.org/10.1016/j.gsf.2013.12.006.

Lybéris, N., 1984. Tectonic evolution of the North Aegean trough. Geol. Soc. London Spec. Pub. 17, 709–725.

Lykousis, V., Sakellariou, D., Moretti, I., Kaberi, H., 2007. Late Quaternary basin evolution of the Gulf of Corinth: sequence stratigraphy, sedimentation, fault-slip and subsidence rates. Tectonophysics 440, 29–51. http://dx.doi.org/10.1016/j.tecto.2006.11.007.

Mansfield, C., Cartwright, J., 2001. Fault growth by linkage: observations and implicationsfrom analogue models. J. Struct. Geol. 23, 745–763.

McCalpin, J.P., 2009. Paleoseismology. 2nd edition. Academic Press (613 pp.).

McKenzie, D., 1972. Active tectonics of the Mediterranean Region. Geophys. J. R. Astron. Soc. 30, 109–185.

McKenzie, D., 1978. Active tectonics of the Alpine–Himalayan belt: the Aegean Sea and surrounding regions. Geophys. J. R. Astron. Soc. 55, 217–254.

McNeill, L.C., Collier, R.E., 2004. Footwall uplift rates of the Eastern Eliki Fault, Gulf of Corinth, Greece, inferred from Holocene and Pleistocene terraces. Geol. Soc. Lond. Spec. Publ. 161, 81–92.

McNeill, L.C., Ll, Collier R.E., 2004. Uplift and slip rates of the eastern Eliki fault segment, Gulf of Corinth, Greece, inferred from Holocene and Pleistocene terraces. J. Geol. Soc. 161, 81–92.

McNeill, L.C., Cotterill, C.J., Henstock, T.J., Bull, J.M., Stefatos, A., Ll, Collier R.E., Papatheoderou, G., Ferentinos, G., Hicks, S.E., 2005. Active faulting within the offshore western Gulf of Corinth, Greece: implications for models of continental rift deformation. Geology 33, 241–244.

Mercier, J.-L., 1977. Principal results of a neotectonic study of the Aegean Arc and its localisation within the Eastern Mediterranean. 6th Colloquium on the Geology of the Aegean Region, Inst. Geol. Min. Expl., Athens, *Proceedings*, III, pp. 1281–1291.

Mercier, J.L., Gailhardis, E.C., 1989. Regional state of stress and characteristic fault kinematics instabilities shown by aftershock sequences: the aftershock sequences of the 1978 Thessaloniki (Greece) and 1980 Campania–Lucania (Italia) earthquakes as examples. Earth Planet. Sci. Lett. 92, 247–264.

Mercier, J.L., Mouyaris, N., Simeakis, C., Roundoyannis, T., Angelidis, C., 1979. Intra-plate deformation: a quantitative study of the faults activated by the 1978 Thessaloniki earthquakes. Nature 278, 45–48.

Mercier, J.-L., Carey, E., Mouyaris, N., Simeakis, K., Roundoyannis, T., Anghelidhis, C., 1983. Structural analysis of recent and active faults and regional state of stress in the epicentral area of the 1978 Thessaloniki earthquakes (Northern Greece). Tectonics 2 (6), 577–600.

Mercier, J.L., Sorel, D., Vergely, P., Simeakis, K., 1989. Extensional tectonic regimes in the Aegean basins during the Cenozoic. Basin Res. 2, 49–71.

Meyer, B., Armijo, R., Massonet, D., De Chabalier, J.-B., Delacourt, C., Ruegg, J.-C., Achache, C., Briole, P., Papanastassiou, D., 1996. The 1995 Grevena (Northern Greece) earthquake: fault model constrained with tectonic observations and SAR interferometry. Geophys. Res. Lett. 23, 2677–2680.

Meyer, B., Armijo, R., Massonnet, D., de Chabalier, J.B., Delacourt, C., Ruegg, J.C., Achache, J., Papanastassiou, D., 1998. Comment on "Geodetic investigation of the 13 May Kozani–Grevena (Greece) earthquake" by Clarke et al. Geophys. Res. Lett. 25, 129–130.

Micarelli, L., Moretti, I., Daniel, J.M., 2003. Structural properties of rift-related normal faults: the case study of the Gulf of Corinth, Greece. J. Geodyn. 36, 275–303.

Molchan, G., Kronrod, T., Panza, G.F., 1997. Multi-scale seismicity model for seismic risk. Bull. Seismol. Soc. Am. 87 (5), 1220–1229.

Mountrakis, D., Psilovikos, A., Papazachos, B., 1983. The geotectonic regime of the 1978 Thessaloniki earthquake. In: Papazachos, B.C., Carydis, P.G. (Eds.), *The Thessaloniki, northern Greece, earthquake of June 20, 1978, and its seismic sequence*, Technical Chamber of Greece-Section of Central Macedonia, pp. 11–27.

Mountrakis D., Kilias A., Pavlides S., Sotiriadis L., Psilovikos A., Astaras Th., Vavliakis E., Koufos G., Dimopoulos G., Soulios G., Christaras V., Skordilis M., Tranos M., Spyropoulos N., Patras D., Syrides G., Lambrinos N. and Laggalis T. (1996): *Neotectonic map of Greece, Langadhas sheet, scale 1:100,000*. Earthquake Planning and Protection Organisation and European Centre on Prevention and Forecasting of Earthquakes.

Mountrakis, D., Pavlides, S., Zouros, N., Astaras, Th., Chatzipetros, A., 1998. Seismic fault geometry and kinematics of the 13 May 1995 western Macedonia (Greece) earthquake. J. Geodyn. 26 (2–4), 175–196.

Mountrakis, D., Tranos, M., Papazachos, C., Thomaidou, E., Karagianni, E., Vamvakaris, D., 2006. Neotectonic and seismological data concerning major active faults, and the stress regimes of Northern Greece. In: Robertson, A.H.F., Mountrakis, D. (Eds.), Tectonic Development of the Eastern Mediterranean Region. *Geol. Soc. London*, Sp. Pub. 260, pp. 649–670.

Mucciarelli, M., 2005. What is a surprise earthquake? The example of the 2002, San Giuliano (Italy) event. Ann. Geophys. 48 (2), 273–278.

Mulargia, F., 2013. Why the next large earthquake is likely to be a big surprise. Bull. Seismol. Soc. Am. 103 (5), 2946–2952. http://dx.doi.org/10.1785/0120130047.

Nekrasova, A.K., Kosobokov, V.G., 2006. General law of similarity for earthquakes: evidence from the Baikal Region. Dokl. Earth Sci. 407A (3), 484–485.

Nekrasova, A.K., Kossobokov, V.G., Peresan, A., Aoudia, A., Panza, G.F., 2011. A multiscale application of the unified scaling law for earthquakes in the Central Mediterranean area and Alpine Region. Pure Appl. Geophys. 168 (1), 297–327.

Nelson, A.R., 1992. Lithofacies analysis of colluvial sediments—an aid in interpreting the recent history of Quaternary normal faults in the Basin and Range Province, Western United States. J. Sediment. Petrol. 62, 607–621.

North, R.G., 1977. Seismic moment, source dimensions, and stress associated with earthquakes in the Mediterranean and Middle East. Geophys. J. R. Astron. Soc. 48, 137–161.

Palyvos, N., Pavlopoulos, K., 2008. Acquisition of data for seismic hazard assessments, with paleoseismological and geomorphological methods. (in Greek), ENTER Proj. 47(04EP47), Gen. Secr. of Res. and Technol, Athens Available at: http://www.hua.gr/geografias/kpavlop/ programmata/2008_04EP47/Main.html.

Palyvos, N., Pavlopoulos, K., Froussou, E., Kranis, H., Pustovoytov, K., Forman, S.L., Minopoulos, D., 2010. Paleoseismological investigation of the oblique-normal Ekkara ground rupture zone accompanying the M 6.7–7.0 earthquake on 30 April 1954 in Thessaly, Greece: archaeological and geochronological constraints on ground rupture recurrence. J. Geophys. Res. 115, B06301.

Panagiotopoulos, D.G., Papadimitriou, E.E., Papaioannou, Ch.A., Scordilis, E.M., Papazachos, B.C., 1993. Source Properties of the 21 December 1990 Goumenissa Earthquake in Northern Greece. 2nd Congress of the Hellenic Geophysical Union, 5–7 May 1993, Florina, Greece, *Proceedings*, pp. 286–296.

Papadopoulos, G.A., 2000. Historical earthquakes and tsunamis in the Corinth Rift, Central Greece. National Observatory of Athens, Institute of Geodynamics, Publ. n. 12 p. 128 (Athens). Q44

Papanastassiou, D., 2001. The Konitsa, Epirus-NW Greece, July 26 (Ms = 5.4) and August 5, 1996, (Ms = 5.7) earthquakes sequence. Bull. Geol. Soc. Greece 34 (4), 1555–1562.

Papastamatiou, D., Mouyiaris, N., 1986. The Sophadhes earthquake occurred on April 30th 1954 — field observations by Yannis Papastamatiou. Geol. Geophys. Res. 341–362 (Sp. Issue).

Papazachos, B.C., 1990. Seismicity of the Aegean and surrounding area. Tectonophysics 178, 287–308.

Papazachos, B.C., Comninakis, P.E., 1982. A catalogue of historical earthquakes in Greece and surrounding area for the period 1901–1980. Geophys. Lab. Univ. of Thessaloniki Publ., University of Thessaloniki, 6 (146 pp, Thessaloniki). Q45

Papazachos, C.B., Kiratzi, A., 1996. A detailed study of the active crustal deformation in the Aegean and surrounding area. Tectonophysics 253, 129–153.

Papazachos, B.C., Papazachou, K., 1989. *Oi seismoi tis Elladas* [The earthquakes of Greece]. Editions ZITI, Thessaloniki (356 pp. [in Greek]).

Papazachos, B.C., Papazachou, C., 1997. The Earthquakes of Greece. Second edition. Editions ZITI, Thessaloniki (304 pp.).

Papazachos, B.C., Mountrakis, D., Psilovikos, A., Leventakis, G., 1979. Surface fault traces and fault plane solutions of the May–June 1978 major shocks in the Thessaloniki area, Greece. Tectonophysics 53, 171–183.

Papazachos, B.C., Comninakis, P.E., Hatzidimitriou, P.M., Kiriakidis, E.C., Kiratzi, A.A., Panagiotopoulos, D.G., Papadimitriou, E.E., Papaioannou, C.A., Pavlides, S., 1982. Atlas of Isoseismal Maps for Earthquakes in Greece 1902–1981. Publ. Geophys. Lab. Univ. Thessaloniki 4 (126 pp.).

Papazachos, B.C., Papaioannou, Ch.A., Papazachos, B.C., Savvaidis, A.S., 1997. Atlas of Isoseismal Maps for Strong Shallow Earthquakes in Greece and Surrounding area (426 BC–1995. Publ. Geophys. Lab. Univ. Thessaloniki 4 (176 pp.).

Papazachos, B.C., Karakostas, B.G., Kiratzi, A.A., Papadimitriou, E.E., Papazachos, C.B., 1998. A model for the 1995 Kozani–Grevena seismic sequence. J. Geodyn. 26, 217–231.

Papazachos, B.C., Papaioannou, C.A., Papazachos, C.B., Savvaidis, A.S., 1999. Rupture zones in the Aegean region. Tectonophysics 308, 205–221.

Papazachos, B.C., Mountrakis, D.M., Papazachos, C.B., Tranos, M.D., Karakaisis, G.F., Savvaidis, A.S., 2001. The faults which have caused the known major earthquakes in Greece and surrounding region between the 5th century BC and today. 2nd Greek Conf. Earthquake Eng. and Eng. Seismology, Thessaloniki, 28–30 September 2001, *Proceedings*, 1, pp. 17–26.

Paradisopoulou, P.M., Karakostas, V.G., Papadimitriou, E.E., Tranos, M.D., Papazachos, C.B., Karakaisis, G.F., 2006. Microearthquake study of the broader Thessaloniki area (Northern Greece). Ann. Geophys. 49 (4/5), 1081–1093.

Pavlides, S., 1993. Active faulting in multi-fractured seismogenic areas; examples from Greece. Z. Geomorphol. 94, 57–72 (*N.F.*,).

Pavlides, S., Caputo, R., 2004. Magnitude versus faults' surface parameters: quantitative relationships from the Aegean. Tectonophysics 380, 159–188.

Pavlides, S.B., Kilias, A.A., 1987. Neotectonic and active faults along the Serbomacedonian zone (SE Chalkidiki, northern Greece). Ann. Tectonicae 1 (2), 97–104.

Pavlides, S.B., Mountrakis, D.M., 1987. Extensional tectonics of northwestern Macedonia, Greece, since the late Miocene. J. Struct. Geol. 9 (4), 385–392.

Pavlides, S.B., Zouros, N.C., Chatzipetros, A.A., Kostopoulos, D.S., Mountrakis, D.M., 1995. The 13 May 1995 western Macedonia, Greece (Kozani Grevena) earthquake; preliminary results. Terra Nova 7, 544–549.

Pavlides, S., Koukouvelas, I., Stamatopoulos, L., Agrafiotis, D., Alexandris, G.-A., Zygouri, B., Sboras, S., 2001. Palaeoseismological investigation of the Eastern 'segment' of the Heliki Fault, Gulf of Corinth, Greece. Bull. Geol. Soc. Greece XXXIV (1), 199–205 (in Greek with English abstract).

Pavlides, S.B., Koukouvelas, I.K., Kokkalas, S., Stamatopoulos, L., Keramydas, D., Tsodoulos, I., 2004. Late Holocene evolution of the East Eliki fault, Gulf of Corinth (Central Greece). Quat. Int. 115–116, 139–154.

Pavlides, S.B., Valkaniotis, S., Chatzipetros, A., 2007. Seismically capable faults in Greece and their use in seismic hazard assessment. 4th Int. Conf. Earthq. Geotech. Eng., June 25–28, 2007, Thessaloniki, *Proceedings*, paper n. 1609.

Pavlides, S., Caputo, R., Sboras, S., Chatzipetros, A., Papathanasiou, G., Valkaniotis, S., 2010. The Greek catalogue of active faults and database of seismogenic sources. Bull. Geol. Soc. Greece 43 (1), 486–494.

Pirazzoli, P.A., Stiros, S.C., Fontugne, M., Arnold, M., 2004. Holocene and Quaternary uplift in the central part of the southern coast of the Corinth Gulf (Greece). Mar. Geol. 212, 35–44.

Please cite this article as: Caputo, R., et al., Comparison between *single-event effects* and *cumulative effects* for the purpose of seismic hazard assessment. A review from Greece, Earth-Sci. Rev. (2015), http://dx.doi.org/10.1016/j.earscirev.2015.05.004

Postpischl D. (Ed.) (1985): Catalogo dei terremoti italiani dall'anno 1000 al 1980. *Quaderni della Ricerca Scientifica*, 114, 2B, 239 pp., Bologna.

Poulimenos, G., Doutsos, T., 1996. Barriers on seismogenic faults in Central Greece. J. Geodyn. 22, 119–135.

Resor, P.G., Pollard, D.D., Wright, T.J., Beroza, G.C., 2005. Integrating high-precision aftershock locations and geodetic observations to model coseismic deformation associated with the 1995 Kozani–Grevena earthquake, Greece. J. Geophys. Res. 110, B09402.

Rietbrock, A., Tiberi, C., Scherbaum, F., Lyon-Caen, H., 1996. Seismic slip on a low angle normal fault in the Gulf of Corinth: evidence from high-resolution cluster analysis of microearthquakes. Geophys. Res. Lett. 23 (14), 1817–1820.

Rigo, A., Lyon-Caen, H., Armijo, R., Deschamps, A., Hatzfeld, D., Makropoulos, K., Papadimitriou, P., Kassaras, 1996. A microseismic study in the western part of the Gulf of Corinth (Greece): implications for large-scale normal faulting mechanisms. Geophys. J. Int. 126, 663–688.

Rigo, A., de Chabalier, J.-B., Meyer, B., Armijo, R., 2004. The 1995 Kozani–Grevena (northern Greece) earthquake revisited: an improved faulting model from synthetic aperture radar interferometry. Geophys. J. Int. 157, 727–736.

Roberts, G.P., Koukouvelas, I., 1996. Structural and seismological segmentation of the Gulf of Corinth fault system: implications for models of fault growth. Ann. Geophys. 39 (3), 619–646.

Roumelioti, Z., Theodulidis, N., Kiratzi, A., 2007. The 20 June 1978 Thessaloniki (Northern Greece) earthquake revisited: slip distribution and forward modeling of geodetic and seismological observations. 4th Int. Conf. Earthq. Geotech. Eng., June 25–28, Paper No. 1594.

Sachpazi, M., Galvé, A., Laigle, M., Hirn, A., Sokos, E., Serpetsidaki, A., Marthelot, J.-M., Pi Alperin, J.M., Zelt, B., Taylor, B., 2007. Moho topography under central Greece and its compensation by Pn time-terms for the accurate location of hypocenters: the example of the Gulf of Corinth 1995 Aigion earthquake. Tectonophysics 440, 53–65.

Sboras, S., 2012. The Greek Database of Seismogenic Sources: seismotectonic implications for North Greece. (Ph.D. Thesis). University of Ferrara, p. 252.

Schmidt, J.F., 1867. Pragmatia peri tou genomenou to 1861 Dec. 26 seismou tou Aigiou. Ethniko Typografio, Athens (52 pp. [in Greek]).

Q46 Schmidt, J., 1879. Studien über Erdbeben. pp. 68–83 (Leipzig, Carl Schottze, Leipzig).

Schwartz, P.D., Coppersmith, K.J., 1984. Fault behaviour and characteristic earthquakes: examples from the Wasatch and San Andreas Fault. J. Geophys. Res. 89, 5681–5698.

Silverii, F., Cheloni, D., D'Agostino, N., Selvaggi, G., Boschi, E., 2014. Post-seismic slip of the 2011 Tohoku-Oki earthquake from GPS observations: implications for depth-dependent properties of subduction megathrusts. Geophys. J. Int. 198 (1), 580–596. http://dx.doi.org/10.1093/gji/ggu149.

Skourtsos, E., Kranis, H., 2009. Structure and evolution of the western Corinth Rift, through new field data from the Northern Peloponnesus. Geol. Soc. London Spec. Pub. 321, 119–138.

Soliva, R., Benedicto, A., 2004. A linkage criterion for segmented normal faults. J. Struct. Geol. 26, 2251–2267.

Sorel, D., 2000. A Pleistocene and still-active detachment fault and the origin of the Corinth–Patras rift, Greece. Geology 28, 83–86.

Soufleris, C., Stewart, G., 1981. A source study of the Thessaloniki (northern Greece) 1978 earthquake sequence. Geophys. J. R. Astron. Soc. 67, 343–358.

Soufleris, C., Jackson, J.A., King, G.C.P., Spencer, C.P., Scholz, C.H., 1982. The 1978 earthquake sequence near Thessaloniki (northern Greece). Geophys. J. R. Astron. Soc. 68, 429–458.

Steacy, S., Jiménez, A., Holden, C., 2014. Stress triggering and the Canterbury earthquake sequence. Geophys. J. Int. 196 (1), 473–480. http://dx.doi.org/10.1093/gji/ggt380.

Stefatos, A., Papatheodorou, G., Ferentinos, G., Leeder, M., Collier, R., 2002. Seismic reflection imaging of active offshore faults in the Gulf of Corinth: their seismotectonic significance. Basin Res. 14, 487–502.

Stewart, I., 1996. Holocene uplift and palaeoseismicity on the Eliki Fault, Western Gulf of Corinth Greece. Ann. Geophys. 39 (3), 575–588.

Stewart, I.S., Hancock, P.L., 1991. Scales of structural heterogeneity within neotectonic normal fault zones in the Aegean region. J. Struct. Geol. 13, 191–204. http://dx.doi.org/10.1016/0191-8141(91)90066-R.

Stiros, S.C., Drakos, A., 2000. Geodetic constrains on the fault pattern of the 1978 Thessaloniki (Northern Greece) earthquake (Ms = 6.4). Geophys. J. Int. 143, 679–688.

Archaeoseismology. In: Stiros, S., Jones, R.E. (Eds.), British School at Athens, Fitch Laboratory occasional paper 7. The Short Run Press (Exeter) 268 pp.

Stucchi, M., Albini, P., Camassi, R., Musson, R.M.W., Tatevossian, R., 2001. Main results of the Project BEECD "A Basic European Earthquake Catalogue and a Database for the evaluation of long-term seismicity and seismic hazard". In: Yeroyanni, M., Margottini, C., Zonno, G. (Eds.), Tools for Planning in Seismic Areas: Integrated Approaches and Data Availability. European Commission Volume, Brussels (http://emidius.mi.ingv.it/BEECD/ (last visited August 2014)).

Suhadolc, P., Moratto, L., Costa, G., Triantafyllidis, P., 2007. Source modeling of the Kozani and Arnea 1995 events with strong motion estimates for the city of Thessaloniki. J. Earthq. Eng. 11 (4), 560–581. http://dx.doi.org/10.1080/13632460601188035.

Taylor, B., Weiss, J.R., Goodliffe, A.M., Sachpazi, M., Laigle, M., Hirn, A., 2011. The structures, stratigraphy and evolution of the Gulf of Corinth rift, Greece. Geophys. J. Int. 185, 1189–1219. http://dx.doi.org/10.1111/j.1365-246X.2011.05014.x.

Taymaz, T., Jackson, J., McKenzie, D., 1991. Active tectonics of the north and central Aegean Sea. Geophys. J. Int. 106, 433–490.

Tranos, M., Papadimitriou, E., Kilias, A., 2003. Thessaloniki–Gerakarou Fault Zone (TGFZ): the western extension of the 1978 Thessaloniki earthquake fault (Northern Greece) and seismic hazard assessment. J. Struct. Geol. 25, 2109–2123.

Utkucu, M., 2013. 23 October 2011 Van, Eastern Anatolia, earthquake (M W 7.1) and seismotectonics of Lake Van area. J. Seismol. 17 (2), 783–805. http://dx.doi.org/10.1007/s10950-012-9354-z.

Database of potential sources for earthquakes larger than M 5.5 in Italy. In: Valensise, G., Pantosti, D. (Eds.), *Ann. Geofisica* 44(4), pp. 797–807.

Valkaniotis S. (2005): Research of active faults in Western Thessaly. M.Sc. thesis, Aristotle University of Thessaloniki, pp. 122 (unpublished, in Greek).

Vannucci, G., Gasperini, P., 2003. A database of revised fault plane solutions for Italy and surrounding regions. Comput. Geosci. 29, 903–909.

Vannucci, G., Gasperini, P., 2004. The new release of the database of Earthquake Mechanisms of the Mediterranean Area (EMMA Version 2). Ann. Geofis. 307–334 (supplement to Vol. 47).

Verrios, S., Zygouri, V., Kokkalas, S., 2004. Morphotectonic analysis in the Eliki Fault zone (Gulf of Corinth, Greece). Bull. Geol. Soc. Greece 36, 1706–1715.

Voidomatis, P., 1989. Some aspects of a seismotectonic synthesis in the North Aegean Sea and surrounding area. Boll. Geofis. Teor. Appl. 31, 49–61.

Voidomatis, Ph.S., Pavlides, S.B., Papadopoulos, G.A., 1990. Active deformation and seismic potential in the Serbomacedonian zone, northern Greece. Tectonophysics 179, 1–9.

Walsh, J.J., Watterson, J., 1991. Geometric and kinematic coherence and scale effects in normal fault systems. Geol. Soc. London Spec. Pub. 56, 193–203. http://dx.doi.org/10.1144/GSL.SP.1991.056.01.13.

Wells, D.L., Coppersmith, J.K., 1994. New empirical relationships among magnitude, rupture length, rupture width, rupture area, and surface displacement. Bull. Seismol. Soc. Am. 84, 974–1002.

Wesnousky, S.G., 1994. The Gutenberg–Richter or characteristic earthquake distribution, which is it? Bull. Seismol. Soc. Am. 84 (6), 1940–1959.

Wesnousky, S.G., 2008. Displacement and geometrical characteristics of earthquake surface ruptures: issues and implications for seismic-hazard analysis and the process of earthquake rupture. Bull. Seismol. Soc. Am. 98 (4), 1609–1632. http://dx.doi.org/10.1785/0120070111.

Wyss, M., Nekrasova, A., Kossobokov, V., 2012. Errors in expected human losses due to incorrect seismic hazard estimates. Nat. Hazards 62 (3), 927–935. http://dx.doi.org/10.1007/s11069-012-0125-5.

Yeats, R., Sieh, K., Allen, C., 1997. The Geology of Earthquakes. Oxford University Press, p. 576.